Gently dipping fracture zones in Paleoproterozoic metagranite, Sweden: Evidence from reflection seismic and cored borehole data and implications for the disposal of nuclear waste

Christopher Juhlin[1] and Michael B. Stephens[2]

Received 14 June 2005; revised 2 May 2006; accepted 12 May 2006; published 6 September 2006.

[1] The Svecokarelian orogen in the coastal area north of Stockholm, central Sweden, is characterized by a complex deformation belt. In this belt, bedrock domains strike WNW-NW, dip steeply, and are affected by high ductile strain. These domains anastomose around tectonic lenses that are up to a few tens of kilometers in length and are a few kilometers wide. The bedrock within the lenses is folded and, in general, affected by lower ductile strain. Site investigations for the disposal of highly radioactive nuclear waste are presently in progress within one of these lenses. Approximately 16 km of high-resolution (10 m source and receiver spacing, 100 channels) seismic data were acquired in 2002 along five separate profiles (2 to 5 km in length) within this lens. In the southeast, reflection orientations are well determined where profiles cross one another. Here, there is a nearly one to one correlation of distinct reflections on the seismic sections with hydraulically conductive fracture zones in cored boreholes, indicating that these fracture zones control the reflectivity. However, smaller lenses of amphibolite within the fracture zones may enhance the reflectivity. The reflections dip gently to the SSE and SE, and the zones in the boreholes are dominated by fractures that show the same dip direction or are subhorizontal. A working hypothesis for the gently dipping fracture zones suggests that these structures formed as minor thrust faults during the later stages of the Svecokarelian orogeny. Mineral fillings and coatings along fractures in these zones indicate later reactivation. The current stress field, a high intensity of fractures in the zones at a high angle to σ_3, high in situ stresses in the bedrock, and rapid glacial unloading with the development of high differential stresses may explain the large volume of groundwater in these zones. The reflection seismic data, in combination with the verifying work presented in the cored borehole data, have steered the subsequent focus in geoscientific studies to the northwestern part of the candidate area.

Citation: Juhlin, C., and M. B. Stephens (2006), Gently dipping fracture zones in Paleoproterozoic metagranite, Sweden: Evidence from reflection seismic and cored borehole data and implications for the disposal of nuclear waste, *J. Geophys. Res.*, *111*, B09302, doi:10.1029/2005JB003887.

1. Introduction

[2] Several previous studies [e.g., *Mair and Green*, 1981; *Juhlin*, 1995; *Bergman et al.*, 2002] have shown that reflection seismic surveying is a potentially useful tool for investigating crystalline bedrock, in conjunction with locating a suitable site for a nuclear waste repository. As of 2002 and continuing to present-day, the Swedish Nuclear Fuel and Waste Management Company (SKB) is carrying out extensive studies at two possible sites in Sweden, Forsmark [*SKB*, 2004a, 2005] in the eastern part of central Sweden and Oskarshamn [*SKB*, 2004b] in southern Sweden (Figure 1). Both sites are situated in the Paleoproterozoic bedrock in the Fennoscandian Shield. Reflection seismic surveys are important components of the investigation program at both sites [*SKB*, 2001; *Juhlin et al.*, 2002, 2004]. Apart from being useful as an aid to locate the repository site, the reflection seismic surveys provide important geological information on bedrock structure in the uppermost few kilometers of the Paleoproterozoic crust in the Fennoscandian Shield. In contrast to most other parts of the shield, where reflection seismic surveying has been performed, but where there are few constraints on the geological interpretations that have been carried out, an ongoing drilling program at both sites allows calibration of the interpretations.

[3] In this paper, we first present the seismic sections at the Forsmark site and provide a general overview of the most important aspects of the data. We then focus on a series of gently dipping reflections in the southeastern part of the site and summarize the results of a 1000 m cored drilling study through them. On the basis of the borehole data, we interpret the source to these gently dipping reflections to be associated with fracture zones that formed during the later part of a Paleoproterozoic orogenic event.

[1]Department of Earth Sciences, Uppsala University, Uppsala, Sweden.
[2]Geological Survey of Sweden, Uppsala, Sweden.

0148-0227/06/2005JB003887$09.00

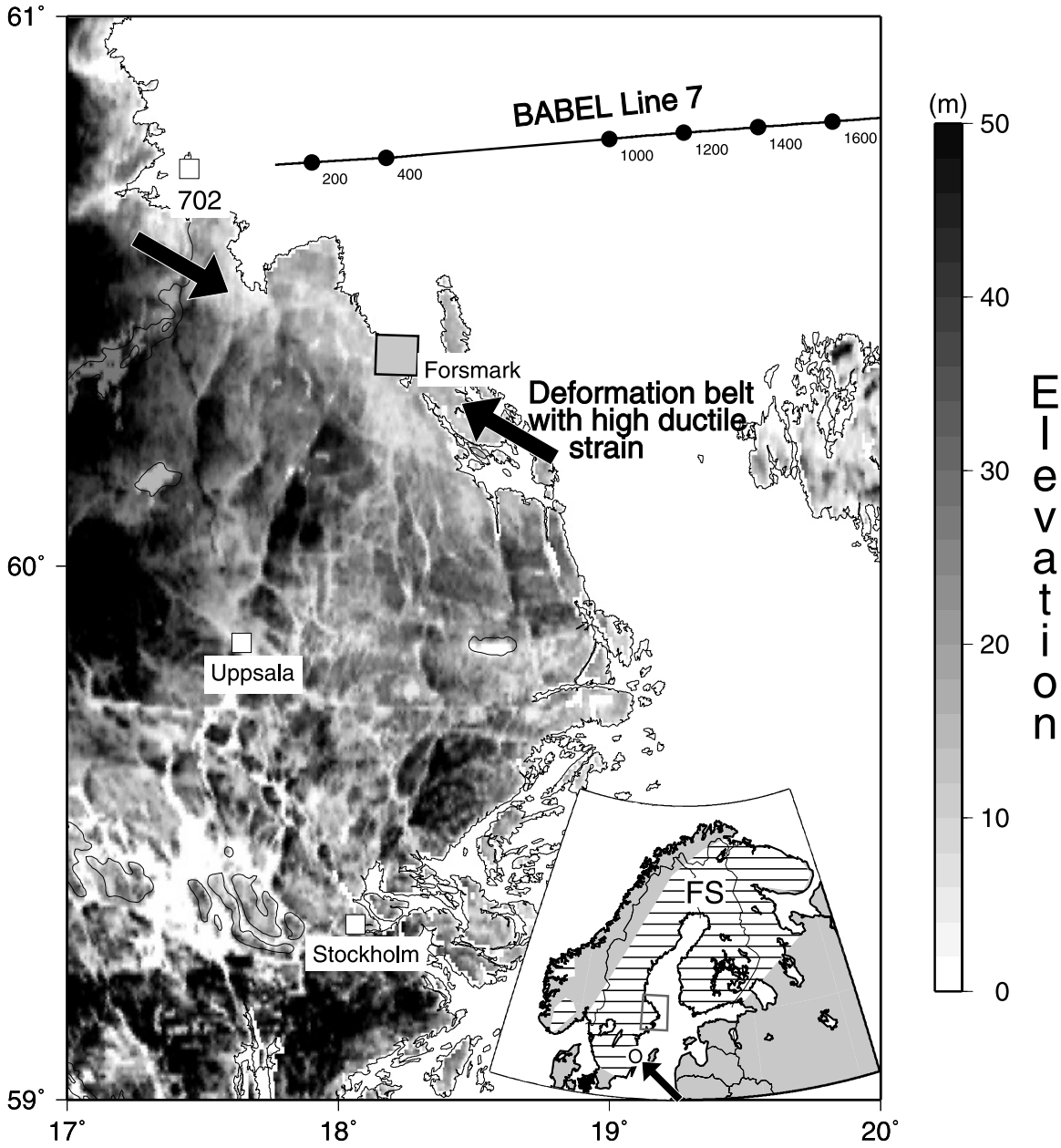

Figure 1. Location of the Forsmark site, Fennoscandian Shield, central Sweden. The coastal deformation belt with high strain (including the Singö shear zone), BABEL line 7, and the land recording array 702 are shown. The Fennoscandian Shield (FS) and the Oskarshamn site in southern Sweden (O as indicated by the arrow) are shown in the inset map.

Small amphibolite lenses within the fracture zones may also enhance the observed reflectivity. We suggest that the present-day stress field favors the reactivation of fractures along these zones as hydraulically active joints. Finally, we discuss how our ability to map these zones with the reflection seismic method, in the southeastern part of the study area, has provided the key geoscientific argument for a focus in ongoing investigations to be carried out in the more seismically transparent northwestern part of the site.

2. Geological Setting

[4] Forsmark is situated in the western part of the Paleoproterozoic Svecokarelian orogen, inside the Fennoscandian Shield (Figure 1). In general, crustal growth and radical crustal reworking in this orogenic system migrated southward and westward during the time interval 1.96 to 1.75 Ga. Younger tectonic events that potentially affected the bedrock in this part of the shield are summarized in Table 1.

[5] A prominent deformation belt characterizes the Svecokarelian orogen along the coastal area north of Stockholm, including the Forsmark site. This belt extends several tens of kilometers across the WNW-NW strike of the rocks. Bedrock domains that dip steeply and are affected by high ductile strain form a conspicuous geological feature of this belt. These domains anastomose around tectonic lenses in

Table 1. Summary of Major, Post-Svecokarelian Tectonic Events, Which Predominantly Affected the Southwestern Part of the Fennoscandian Shield and the Phanerozoic Rocks Around Its Margins[a]

Time Interval	Tectonic Event
1.70–1.56 Ga	Gothian orogenic event [*Gaál and Gorbatschev*, 1987]
Mesoproterozoic	Subsidence
1.46–1.42 Ga	Hallandian orogenic event [*Gaál and Gorbatschev*, 1987]
1.10–0.90 Ga	Sveconorwegian (Grenvillian) orogenic event followed by subsidence [*Gaál and Gorbatschev*, 1987]
Late Neoproterozoic	Extension related to the opening of the Iapetus Ocean and subsidence
Ordovician to Devonian	Caledonian orogeny followed by subsidence [*Gee and Sturt*, 1985; *Stephens*, 1988]
Carboniferous-Permian	Extension
Mesozoic	Extension
Late Cretaceous	Alpine orogenic event [*Coward et al.*, 1989; *Ziegler*, 1987]
Paleocene	Extension related to the opening of the North Atlantic Ocean
Mid Miocene to present	Compression with maximum horizontal stress direction oriented NW
Pleistocene and Holocene	Glacial subsidence followed by unloading and ongoing isostatic rebound

[a]Brittle deformation related to far-field effects of these events is potentially of significance inside the shield (based on the work by *SKB* [2004a, 2005]).

which the bedrock is folded and, in general, affected by lower ductile strain. The northwestern part of one of these tectonic lenses, sited to the southeast of the nuclear power plant at Forsmark (candidate area in Figure 2), is the focus of site investigations to determine a repository for the disposal of Sweden's highly radioactive nuclear waste.

[6] An older suite of calc-alkaline plutonic rocks that formed during the time interval 1887 to 1862 Ma [*Page et al.*, 2004] dominates the bedrock at the Forsmark site [*Stephens et al.*, 2003a]. A metagranite within this suite forms the principal lithology in the candidate area. Amphibolite dikes and minor intrusions of a younger calc-alkaline suite that formed during the time interval 1867 to 1846 Ma [*Page et al.*, 2004] form subordinate rock types [*Stephens et al.*, 2003a]. The planar mineral fabric within the metagranite is folded, with the development of a strong, linear mineral fabric parallel to the fold axis lineation. The marginal areas to the southwest and northeast of the tectonic lens generally show high ductile strain with the development of a tectonic banding parallel to the WNW-NW strike of the rocks (Figure 2).

[7] In accordance with other Precambrian shield areas, a complex network of discrete, ductile and brittle deformation zones transect the Paleoproterozoic rocks at Forsmark. An integrated study of data obtained from surface outcrops, boreholes, airborne geophysical measurements, and digital topographic information show that several, well-defined sets of steeply dipping, ductile and brittle deformation zones intersect the surface [*SKB*, 2004a, 2005].

[8] Zones with WNW and NW strike define the regionally most important set (Figure 2). They show both ductile and brittle deformation, can be traced up to several tens of kilometers along the coastal region, and are prominent on both sides of the candidate area. The zones with NW strike (e.g., Eckarfjärden deformation zone) form splays off the more regionally significant zones with WNW strike (e.g., Forsmark and Singö deformation zones). The Singö deformation zone represents the northwestern extension of the Singö shear zone [*Talbot and Sokoutis*, 1988, 1995]. Drilling through the Eckarfjärden zone has shown that this zone dips steeply toward the southwest [*SKB*, 2005]. Mylonites as well as epidote, quartz and chlorite, which form mineral fillings along fractures, are prominent. These features, in combination with the ^{40}Ar-^{39}Ar hornblende and biotite cooling ages at the site [*Page et al.*, 2004], suggest that the WNW-NW set of deformation zones initiated their development between 1834 Ma and 1704 Ma, probably during the waning stages of the Svecokarelian orogeny.

[9] A second set of solely brittle deformation zones that strike NE, dip steeply, and show traceable lengths less than five kilometers transect the candidate area. These fracture zones formed after the WNW-NW set, against which they terminate. Laumontite, calcite and adularia are prominent as mineral fillings along the fractures in these zones. The conspicuous presence of laumontite indicates that they either formed or were reactivated under lower temperature conditions than the WNW-NW set [*Sandström et al.*, 2004; *SKB*, 2005]. A subordinate, third set of steeply dipping fractures and minor fracture zones with NNW strike is also present at the site.

[10] A critical question that provoked the reflection seismic study was to investigate the occurrence of gently dipping structures at the Forsmark site. Such structures had been encountered in previous construction work [e.g., *Carlsson and Christiansson*, 1987] and are not easy to detect using only standard geological and geophysical, surface data. Furthermore, it was deemed necessary to understand the geological relationships between the established, steeply dipping deformation zones and any gently dipping zones.

3. Data Acquisition

[11] Data acquisition was carried out from March to May during 2002. Approximately 16 km of high-resolution (Table 2) reflection seismic data were acquired along five different profiles (Figure 3) using about 1300 shot points. Most of these shots were also recorded on a stationary network of 11 Orion three-component seismometers, in order to provide deeper velocity information [*Juhlin et al.*, 2002]. However, in this paper we focus on the results from the reflection seismic component of the survey.

[12] Shot points and geophones were located as frequently as possible on the bedrock. Shot holes were drilled at the closest suitable location to a staked point where bedrock was present, but not further from the staked point than 30 cm

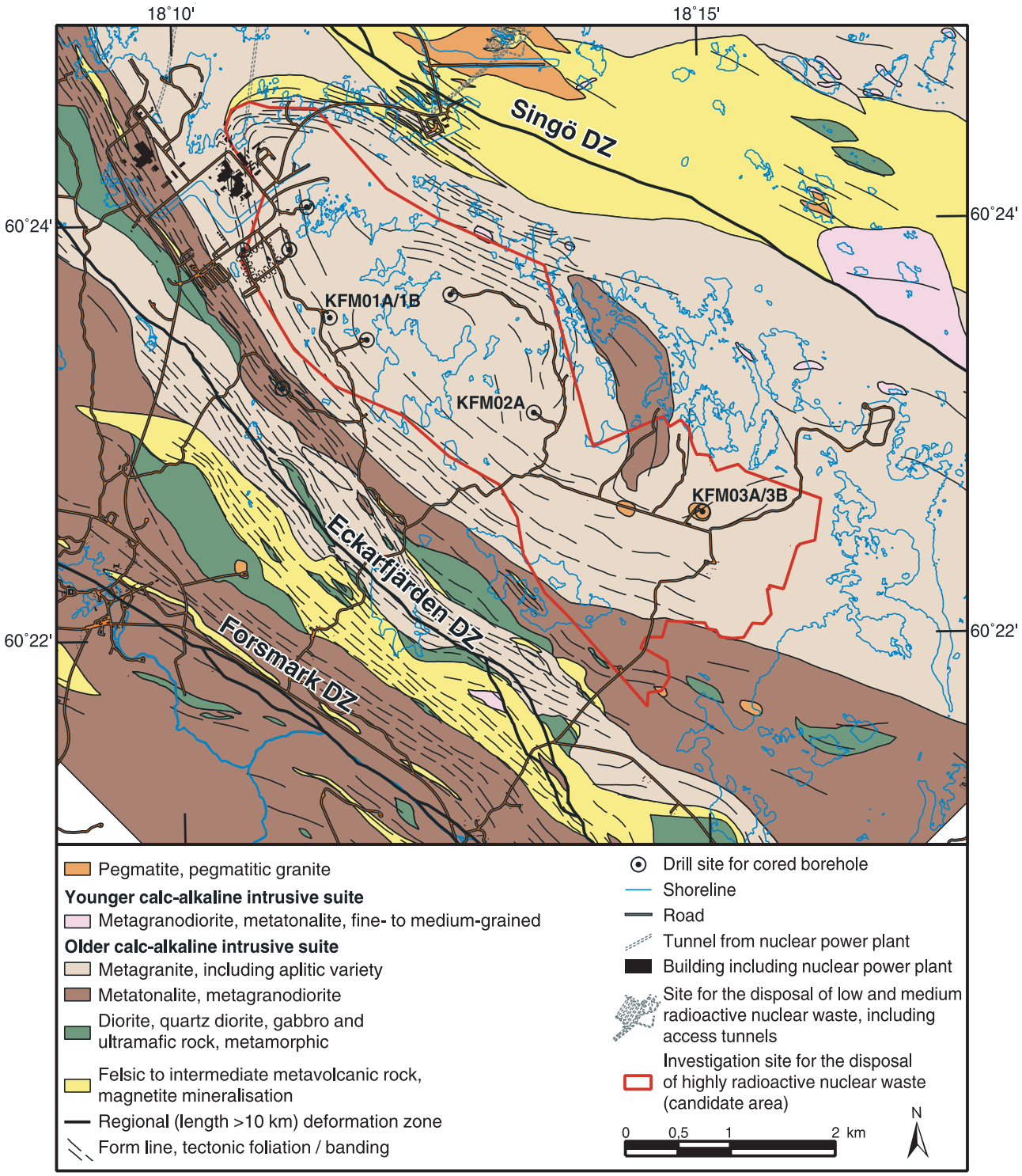

Figure 2. Bedrock geological map of the candidate area and surroundings at the Forsmark site. The locations of the cored boreholes drilled up to the end of 2005 are also shown on this map (extracted from SKB GIS database: Bedrock geological map, Forsmark, version 1.2).

parallel to and 1 m perpendicular to the profile. If no bedrock was found within this area, even after removing 50 cm of Quaternary cover, the shot hole was drilled at the staked point. In the bedrock, 12 mm diameter shot holes were drilled to 90 cm depth with an electric drilling machine powered by a gasoline generator. Charges of 15 g were used in bedrock shot holes. In the Quaternary cover, 32 mm diameter shot holes were drilled to 150 cm depth with an air pressure drill. These holes were cased with a plastic or metal casing with an inner diameter of 16.9 mm (plastic) or 18 mm (metal). Charges of 75 g were used in these holes. Bedrock shot holes were used on only about 5% of the

Table 2. Data Acquisition Parameters

Parameter	Reflection
Spread type	end-on, shoot through
Number of channels	100
Near offset	20 m
Geophone spacing	10 m
Geophone type	28 Hz single
Shot spacing	10 m
Charge size	15/75 gram
Nominal charge depth	0.9/1.5 m
Nominal fold	50
Recording instrument	SERCEL 348
Sample rate	1 ms
Field low cut	8 Hz
Field high cut	250 Hz
Record length	4 s
Profile length/shots	1, 2950 m/260
	2, 2740 m/217
	3, 2050 m/143
	4, 2410 m/196
	5, 5280 m/507

profiles. Wherever possible, geophones were placed in drilled bedrock holes, otherwise they were placed directly in the Quaternary cover. All shot holes and geophone locations were surveyed with high-precision GPS instruments in combination with a total station. This combination gave a horizontal and vertical precision of better than 10 cm.

4. Data Processing

[13] The reflection seismic data were acquired along crooked lines. CDP (common data point) stacking lines were chosen that were piecewise straight. The data were projected onto the lines prior to stacking. In the stacks that follow, CDP number refers to location along these piecewise straight lines. Station numbers are also shown on the stacks, but these are only approximate. Processing parameters were chosen based on previous experience from similar areas [e.g., *Bergman et al.*, 2002]. Important pro-

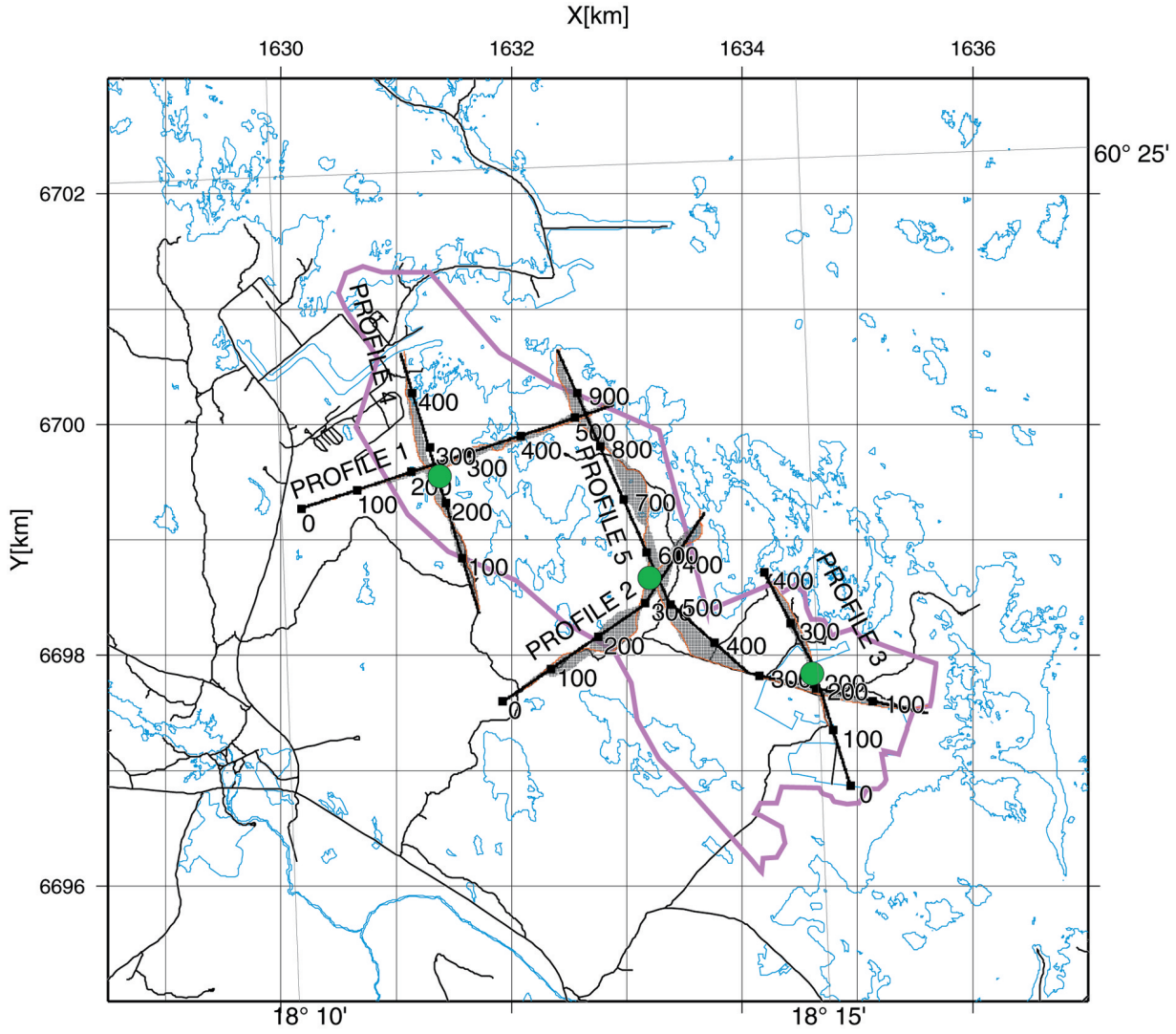

Figure 3. Midpoints between shots and receivers (gray areas) and the common data point (CDP) lines (black lines) along which the reflection seismic data have been projected for stacking and interpretation. The locations of the seismic profiles (red lines) and the near-vertical cored boreholes KFM01A/KFM01B, KFM02A, and KFM03A/KFM03B (green circles) are also shown [after *Juhlin et al.*, 2002]. The candidate area is shown with the heavy purple line.

cessing steps included refraction statics, spectral whitening and dip moveout (DMO). Good refraction statics are critical for successful processing of this type of data [e.g., *Wu and Mereu*, 1992; *Juhlin*, 1995]. The approximate depth scale shown in the unmigrated sections in this paper is based on an average velocity of 5850 m/s. It is only valid for true subhorizontal reflections, not for dipping or out-of-the-plane reflections.

[14] The results and initial interpretation of the reflection seismic study were presented to SKB during 2002 [*Juhlin et al.*, 2002]. A minor reevaluation of the data was recently reported to SKB [*Juhlin and Bergman*, 2004].

5. Results

5.1. Overview of Profiles

[15] First, we present a general overview of the seismic profiles. We then focus on the results from the southeastern part of the study area where prominent reflectors are present in the uppermost crust. We focus on the uppermost 0.3 s (~900 m), since the deep boreholes in the study area penetrate to approximately this level.

[16] Where profiles intersect, it is possible to orient reflections and determine their true strike and dip. Planar surfaces have been fitted by trial and error to the most prominent reflections and the orientation of these planes are provided in Table 3. On the basis of their orientation, the reflections have been grouped into various sets [*Juhlin et al.* 2002; *Juhlin and Bergman*, 2004]. This paper focuses attention on sets A and B that dominate in the southeastern part of the area and are gently dipping. Set A shows an ENE strike direction whereas set B strikes more to the NE. Furthermore, the reflectors in set A intersect the surface, while the set B reflectors generally fail to reach the surface. When the reflections are clear and relatively planar, their orientation can be determined fairly accurately, i.e., ±5 degrees for the strike and a few degrees for the dip of the gently dipping reflections.

[17] The most prominent feature in the northwestern part of the study area is the A1 reflection on profile 4 (Figure 4). On intersecting profile 1, the reflection correlates with subhorizontal events, implying that the reflection originates from nearly within the plane of profile 4. It projects to the surface about 1 km north of the northern end of profile 4, close to the surface trace of the Singö deformation zone. However, its strike differs from the Singö zone. Below reflection A1, strong subhorizontal reflections are present on profiles 1 and 4 at 1–1.2 s (Figure 4). These reflections appear to be ubiquitous on all the profiles (Figures 4 and 5) but are less clearly imaged on profiles 2, 3, and 5. The only clear reflection in the upper 0.3 s on profiles 1 and 4 is the gently, south dipping one marked as A2? on profile 4 (Figure 4). This reflection cannot be oriented, since profile 1 intersects profile 4 to the north of where the reflector is predicted to intersect the surface. Further to the southeast, on the northeastern half of profile 2, several clear reflections are present in the upper 0.3 s.

[18] Clear reflections that dip gently to the SSE and SE are present in the upper 0.3 s of profiles 3 and 5 in the southeastern part of the study area (Figure 5). These reflections can be traced along all of profile 3 and along most of profile 5, but they disappear or become diffuse northwest of CDP 750 on profile 5. Nearly all of the reflections can be correlated across the intersecting profiles 3 and 5 (Figure 6). Attention is focused below on these well-defined reflections.

5.2. Migration Considerations

[19] Fitting of planar surfaces to the seismic data (Figure 6) allows the orientation of the reflecting surfaces to be determined in the vicinity of where the profiles cross one another or where they are sufficiently crooked [e.g., *Ayarza et al.*, 2000; *Zalewski et al.*, 1997]. These planes may then be projected into boreholes (Figure 7) or up to the surface (Figure 8) and compared with other geological and geophysical data. They may also be migrated in three dimensions to the approximately correct spatial position of the reflecting interface [*Cosma et al.*, 2003] and compared to borehole data and geological models. These comparisons provide important constraints on the geological structures that give rise to the reflections. However, the process of selecting prominent reflections is somewhat subjective. Weaker, yet significant reflections may be overlooked. Mapping of the seismic sections to depth and direct comparison with borehole results is preferable. Migration of seismic data is one such mapping method. However, the present data set consists of two-dimensional (2-D) profiles acquired over a 3-D network of reflectors, which implies that most of the reflections are from out-of-the-plane of the profiles. In order to properly migrate all reflections to their true spatial position, 3-D data are required.

[20] In the absence of 3-D data, there are number of options available for migrating 2-D seismic wavefield data in a 3-D world. *Nedimovic and West* [2003] suggest that when the 2-D profile is crooked enough, it can be considered as a swath data set so that coherent reflections can be migrated in three dimensions to their correct spatial positions. This strategy was applied with success on 2-D crooked line data from a mining camp in Canada [*Nedimovic and West*, 2002]. However, the Forsmark profiles are generally not crooked enough for this approach to work and other options need to be considered. Inspection of where the selected reflectors intersect the surface (Figure 8) shows that the set A reflectors generally strike nearly perpendicular to profile 3 and the set B reflectors generally strike nearly perpendicular to the southeastern part of profile 5. Migration tests on synthetic data show that, when reflections strike 75°–90° to the direction of the profiles, then those with dips of 30° or less migrate to within a few meters of their true depth along the profiles, down to depths of 1000 m. Therefore the set A and B reflections should migrate to approximately their correct depths along profile 3 and the southeastern part of profile 5, respectively (Figures 9 and 10). This implies that standard 2-D migration routines [*Yilmaz*, 1987] can be applied along these profiles.

5.3. Correlation With the Cored Boreholes KFM03A/KFM03B

[21] Up to the end of 2005, nearly 11,000 m of cored boreholes have been drilled at nine separate sites in the Forsmark area (Figure 2), in conjunction with the site investigation program. The two cored boreholes KFM03A and KFM03B are of particular relevance in the present study. They are located along profile 3, close to the

Table 3. Orientation of the Most Prominent Reflectors Based on the Work by *Juhlin et al.* [2002][a]

Reflector	Strike	Dip
A1	75	45
A2	80	22
A3	50	23
A4	65	25
A5	75	30
A6	75	30
A7	55	23
B1	30	25
B2	30	25
B3	30	21
B4	50	28
B5	50	25
B6	30	32
B7	25	20

[a]Note that the orientation of reflector A3 was modified slightly following a reevaluation of the seismic data [*Juhlin and Bergman*, 2004]. Furthermore, reflectors A7, B6, and B7 were recognized during this reevaluation.

intersection with profile 5 (Figure 3). These boreholes were drilled during 2003, following acquisition and initial interpretation of the surface reflection seismic data. Predictions that addressed where these reflections were expected to intersect the boreholes were completed prior to the drilling.

[22] Boreholes KFM03A and KFM03B were drilled subvertically (85°), at a distance of ~10 m from each other at the same site [*Claesson and Nilsson*, 2004]. The drilling was carried out with a diameter of 76–77 mm and provided 1001 m of cored borehole. The position of the base of KFM03A corresponds to −988 m (height with respect to sea level). Geophysical logging [*Nielsen and Ringgaard*, 2004] as well as radar and TV logging [*Gustafsson and Gustafsson*, 2004] were completed after the drilling. This was followed up by an interpretation of the geophysical logs [*Thunehed*, 2004] and detailed geological mapping of the borehole [*Petersson et al.*, 2004]. An integrated assessment of all these geological and geophysical data [*Carlsten et al.*, 2004] yielded a synthesis of the rock units and deformation zones that were intersected in the two boreholes (Figure 7). Various measurements of hydraulic transmissivity and hydrogeochemical studies have also been carried out in these boreholes.

[23] The mappable rock units and deformation zones in boreholes KFM03A/KFM03B have been documented by *Carlsten et al.* [2004]. Medium-grained, equigranular metagranite dominates these two boreholes (Figure 7). This rock type is associated with pegmatitic granite in the upper ~100 m. Other mappable units include medium-grained metatonalite, in the borehole interval 220–293 m, and fine- to medium-grained metatonalite, in part associated with pegmatitic granite, in the borehole interval 293–399 m. Amphibolite, fine- to medium-grained metatonalite, pegmatitic granite, and fine- to medium-grained granite, which

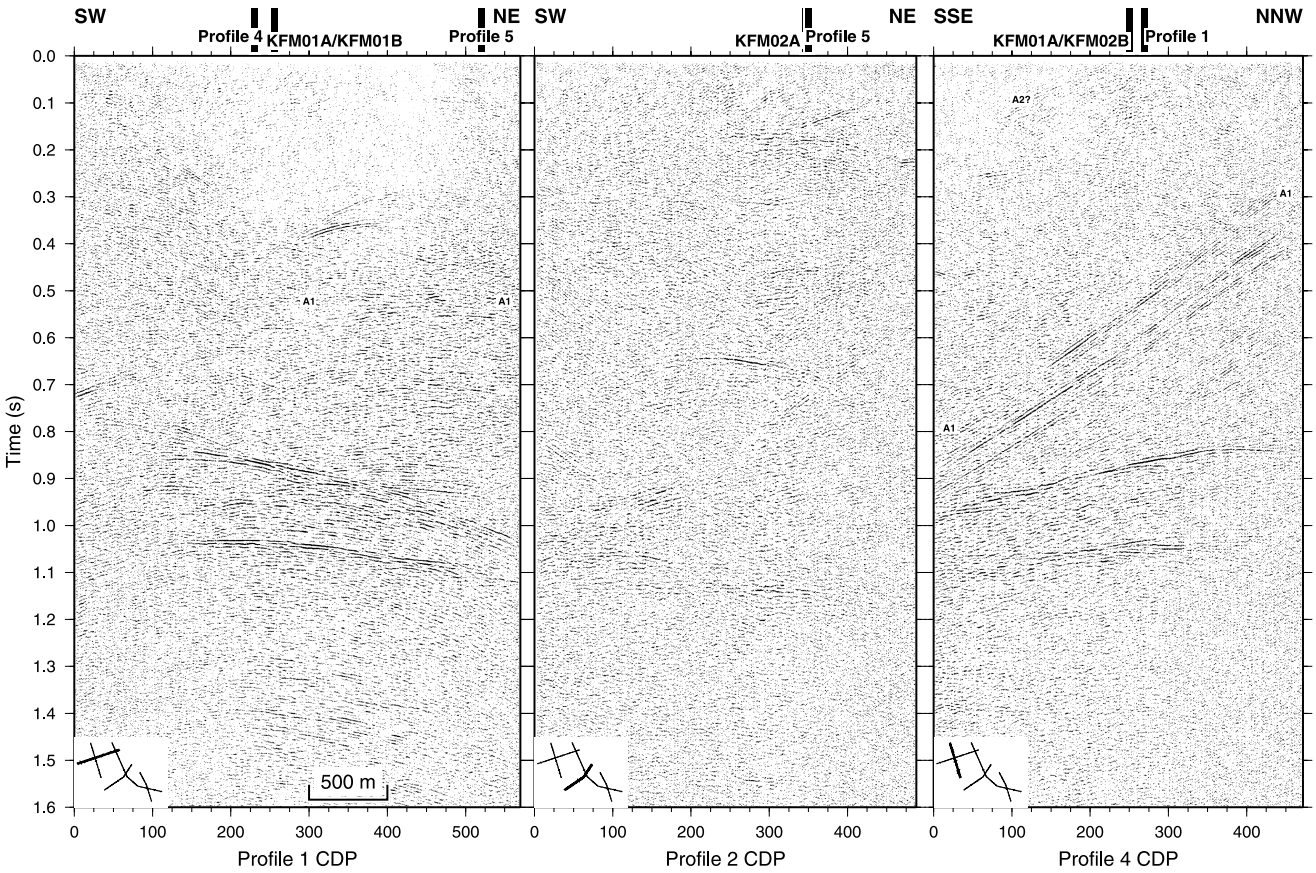

Figure 4. Stacked sections down to 1.6 s for profiles 1, 2, and 4. Index map in the lower left-hand corner of each section shows the location of the profile (thick line) relative to the other profiles (thinner lines) of the survey.

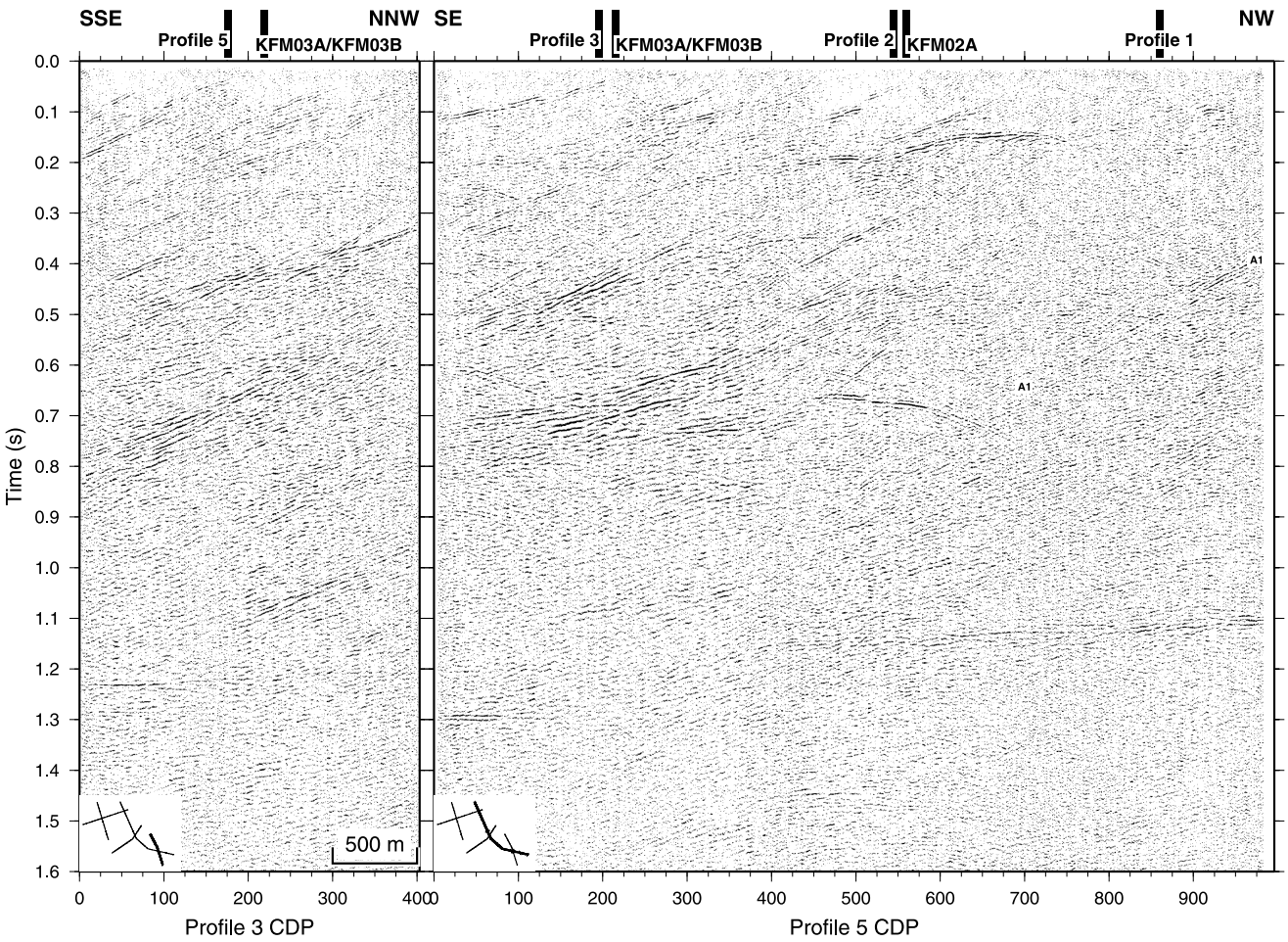

Figure 5. Stacked sections down to 1.6 s for profiles 3 and 5. Index map in the lower left-hand corner of each section shows the location of the profile (thick line) relative to the other profiles (thinner lines) of the survey.

are not shown in Figure 7, occur throughout the boreholes as subordinate (<5 m) components.

[24] Fracture zones have been identified in the borehole intervals 24–42 m, 62–67 m, 356–399 m, 448–455 m, 638–646 m, 803–816 m, and 942–949 m (Figure 7). They have been recognized on the basis of a radically increased frequency of fractures, an increased degree of bedrock alteration, and the presence of one or more geophysical anomalies, including, for example, low P wave velocity [*Carlsten et al.*, 2004]. Amphibolite that is less than 1.5 m in thickness is present within the fracture zones at the borehole intervals 448–455 m and 638–646 m. One or more amphibolites that are only 1–2 dm thick are also present along the remaining zones. Modeling work has integrated the fixed point intersections for the fracture zones with similar intersections in the cored borehole KFM02A (Figure 2) and a number of shallower, percussion boreholes in the vicinity of drill site 3 [*SKB*, 2005].

[25] The fracture zones in KFM03A/KFM03B are dominated by gently dipping fractures that dip to the SSE and SE or are subhorizontal. Both open and sealed fractures are present. The frequency of fractures varies considerably within each zone, maximum values for fracture frequency ranging between 10 and 21 fractures per meter. Thickness estimates, which include both the transitional part and the strongly fractured core part of a zone, vary between 6 and 25 m. The bedrock within the zones is partly altered, with the development of a fine dissemination of hematite grains. Mineral fillings and coatings along the fractures are dominated by chlorite, calcite and clay minerals with subordinate occurrences of quartz, prehnite, laumontite and epidote. In modeling work, these inferred, gently dipping zones have been truncated against steeply dipping zones with WNW and NW strike. On this basis, the gently dipping zones are inferred to vary in length at the surface between ~1.2 and 4 km.

[26] Groundwater flow has been identified along fractures within the fracture zones at the 356–399 m, 448–455 m, 638–646 m, 803–816 m, and 942–949 m borehole intervals. Transmissivity values in the ranges 10^{-9} to 10^{-4} m^2/s, 10^{-9} to 10^{-5} m^2/s, 10^{-8} to 10^{-5} m^2/s, 10^{-8} to 10^{-7} m^2/s, and 10^{-8} to 10^{-6} m^2/s, respectively, have been registered along these zones [*Forsman et al.*, 2004]. The two fracture zones at 24–42 m and 62–67 m appear to be sealed by glacial sediment and no groundwater transmissivity values could be recorded at these two levels. Only in the interval 100–130 m are there high transmissivity values that cannot

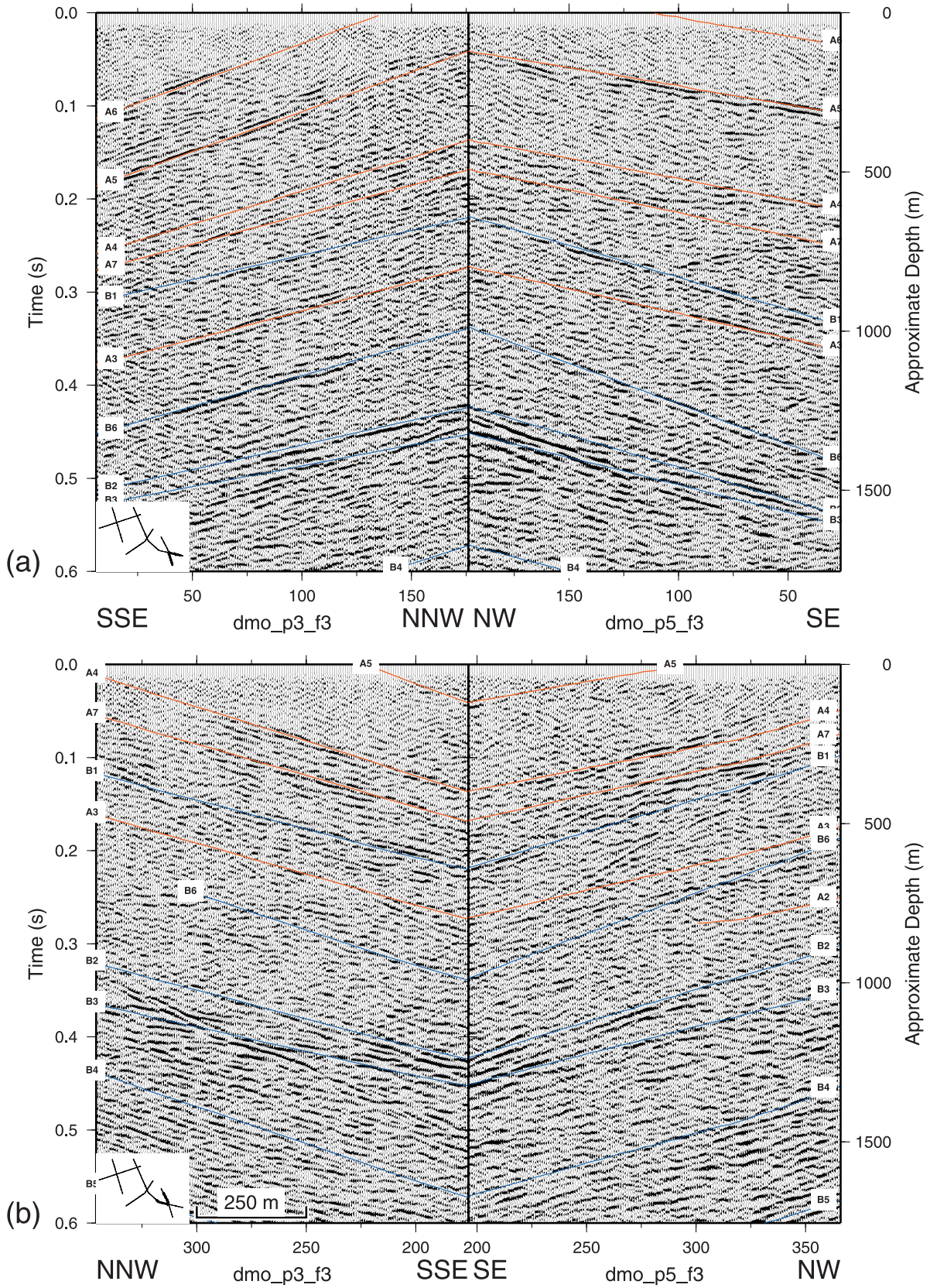

Figure 6. Parts of profiles 3 and 5 viewed from (a) the southeast and (b) the northwest. Selected reflections are marked with lines (red, set A reflections; blue, set B reflections).

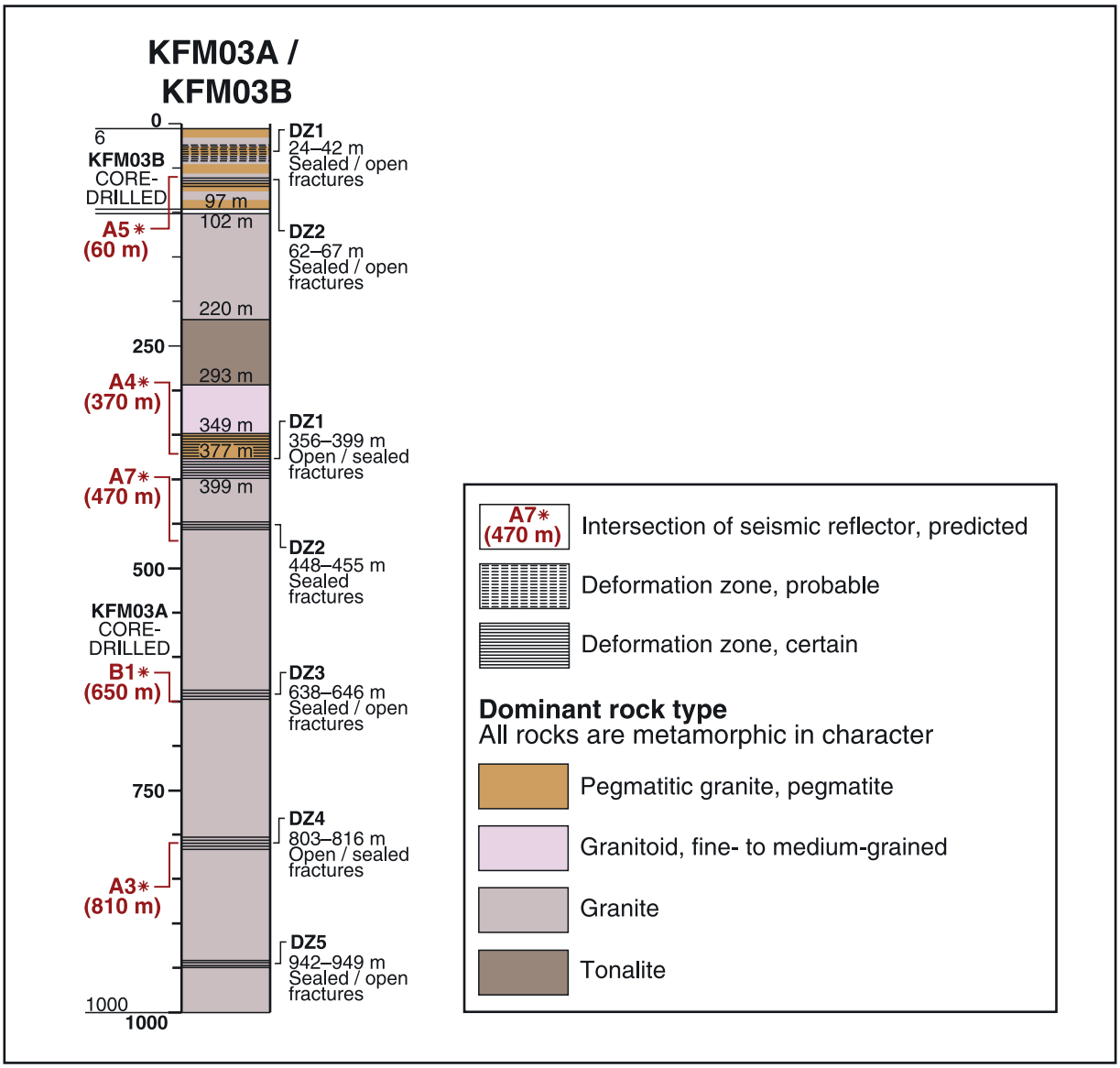

Figure 7. Compilation of rock units and fracture zones (DZ1, DZ2, etc.) in KFM03A and KFM03B, inferred from an integrated assessment of borehole geological and geophysical data (based on the work by *Carlsten et al.* [2004]). The predicted intersections for the reflectors A3, A4, A5, A7, and B1 (based on the work by *Juhlin and Bergman* [2004]) are also shown.

be associated directly with an identified fracture zone or seismic reflector.

[27] On the basis of their favorable orientation, it is predicted that the set A reflections should migrate close to their correct spatial position along profile 3. This is confirmed by comparing the location of the high-amplitude reflections on the migrated section of profile 3 with the projections of the reflectors on to the section (Figure 9). The reflector orientations were estimated from the time sections (Figure 6). The high-amplitude set A reflections coincide closely to the projected depths for the reflectors. The A5, A4, A7 and A3 reflectors intersect boreholes KFM03A/KFM03B where fracture zones have been identified (Figures 7, 9, and 11). Since the B1 reflection emanates from more of out-of-the-plane of profile 3, it migrates to about 100 m shallower than where it is projected to intersect the profile (Figure 9). However, its projection into the borehole corresponds closely to the location of the fracture zone at 638–646 m (Figures 7, 9, and 11).

[28] Only the fracture zone at 942–949 m is not associated with a clear, high-amplitude reflection that was identified prior to drilling. At first inspection, the dipping reflection just below the bottom of borehole KFM03A appears to be a likely candidate reflection that corresponds to this zone (Figure 9). However, this reflection corresponds to B6, which also emanates from out-of-the-plane of profile 3. For this reason, it migrates to a shallower depth than where it is projected to intersect the profile (Figure 9). Drilling of borehole KFM03A approximately 100 m deeper would have yielded an intersection with the B6 reflector. On

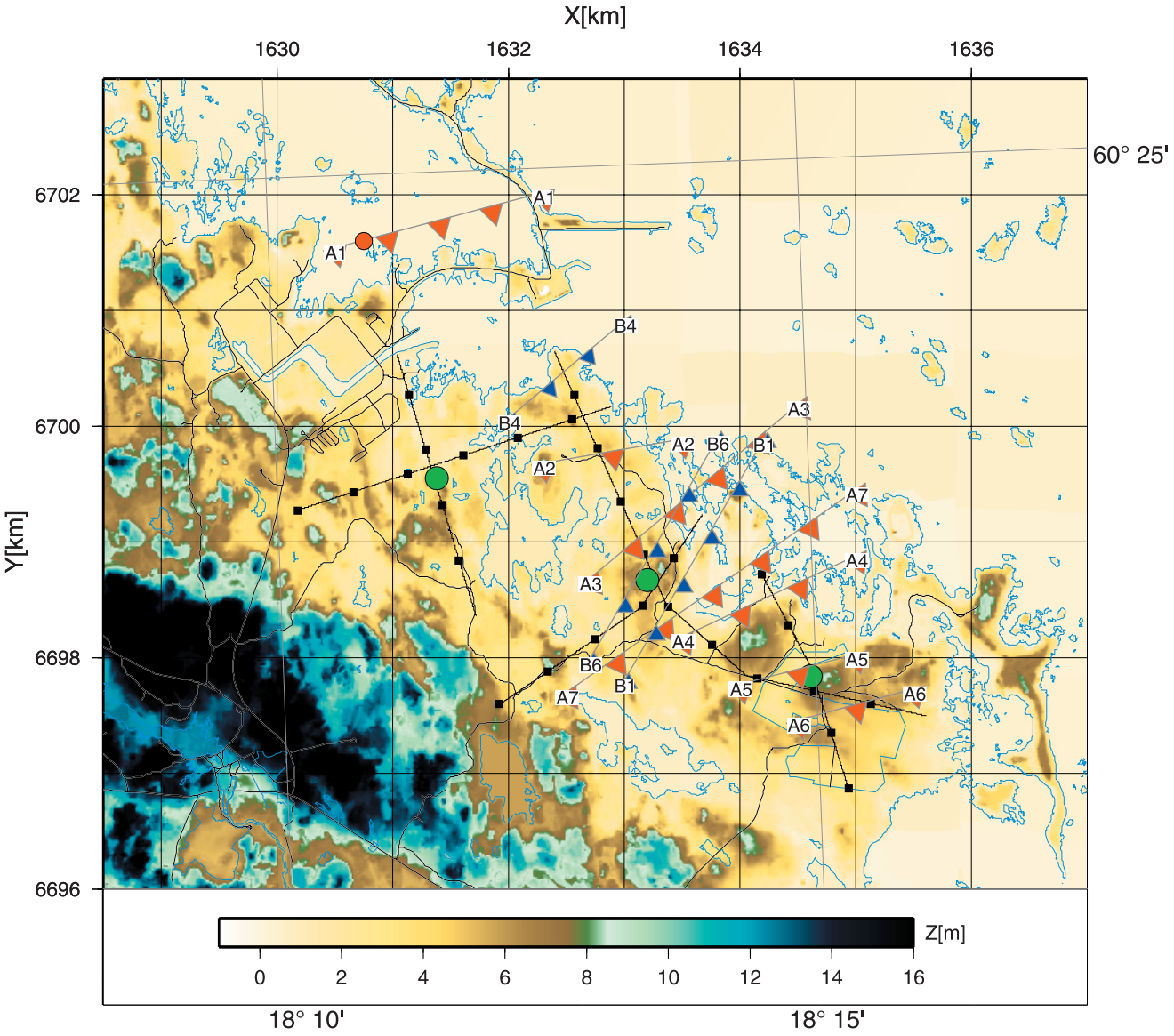

Figure 8. Reflectors projected to the surface and plotted onto a topographic map based on data of *Wiklund* [2002]. Green circles mark the locations of the near-vertical cored boreholes KFM01A/KFM01B, KFM02A, and KFM03A/KFM03B. Where the set A and set B reflectors can be traced to the surface, they are marked with the symbol on the downdip side. A red dot marks where the A1 reflector projects to the surface. Note the consistent SSE and SE dip of the reflectors.

profile 5 (Figure 10) a weak reflection is observed intersecting the borehole at about 950 m. It may represent the conductive fracture zone in the borehole and would belong to the set B reflections. Its average thickness may be too thin or its average impedance contrast may be too low for it to be imaged well on the surface seismic data.

[29] A comparison of the migrated section of profile 5 with the borehole results (Figure 10) shows poorer correspondences than those seen on profile 3. This is due to the set A reflections emanating from more of out-of-the-plane of the profile and that the borehole is offset from profile 5 by about 100 m (Figure 8). However, the B1 and B6 reflections migrate approximately to where they are expected to intersect the profile. From the migrated version of profile 5, it is clear that the B6 reflector was not penetrated by borehole KFM03A.

6. Discussion

6.1. Source of Reflectivity

[30] The strong correlation between the fracture zones identified in the core and the expected intersection depths of the most prominent reflections strongly suggests that these reflections are coupled to the fracture zones themselves. However, inspection of the density and sonic logs (Figure 11) shows that there are numerous points in the borehole where high-density bodies of amphibolite are present, in addition to the low-velocity zones interpreted to be associated with open fractures. Average sonic and density values for the

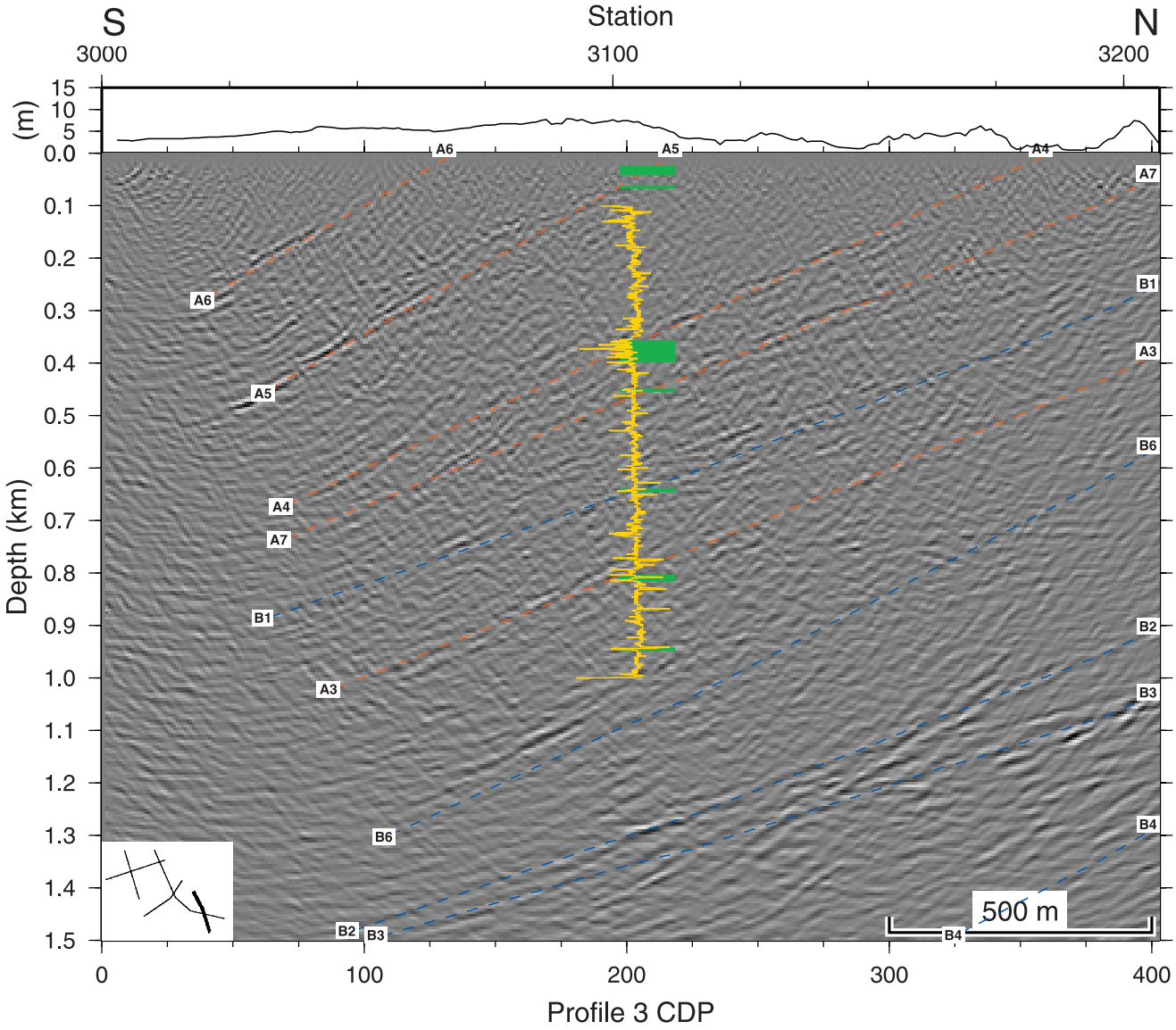

Figure 9. Migrated section of profile 3. P wave velocity geophysical log from the KFM03A borehole [*Nielsen and Ringgaard*, 2004] is shown in yellow, and fracture zones [*Carlsten et al.*, 2004] are indicated in green. Depths of the selected set A (red) and set B (blue) reflectors have been projected into the section. The depths of these reflectors correspond to the depths where the reflectors would be intersected if a borehole were to be drilled along the profile. They should be viewed as true depths. Migration was done with Kirchhoff depth migration using the DMO velocities with which the stacked section was processed.

amphibolites versus intact metagranitic rocks give a higher reflection coefficient compared to average values for the fracture zones versus the intact rock (Table 4), suggesting that the amphibolites can be responsible for the set A and set B reflections in this area. Synthetic seismograms generated using just the density log also give a somewhat better correspondence to the real data than those generated using only the velocity log (Figure 11). Furthermore, dolerite sills in granitic rock are known to produce high-amplitude reflections in the Fennoscandian Shield [*Juhlin*, 1990].

[31] In spite of these observations, we interpret the fracture zones to be the controlling factor in producing the prominent reflections in the southeast. We base this on (1) the previously mentioned correlation between the seismics and the fracture zones in borehole KFM03A, (2) the orientation of the open fractures in the fracture zones have the same orientation as the reflectors, (3) the established hydraulic conductivity on the kilometer scale between boreholes along the fracture zones, and (4) the lack of any large amphibolite bodies mapped on the surface that could produce reflections. The latest point is important since, even if the amphibolites have a greater impedance contrast to the intact metagranite than the fracture zones, they are not likely to extend laterally very far from the borehole. However, locally they are likely to enhance the reflectivity within or close to the fracture zones. It is possible that the amphibolite lenses controlled the geometry of the fracture zones when they formed,

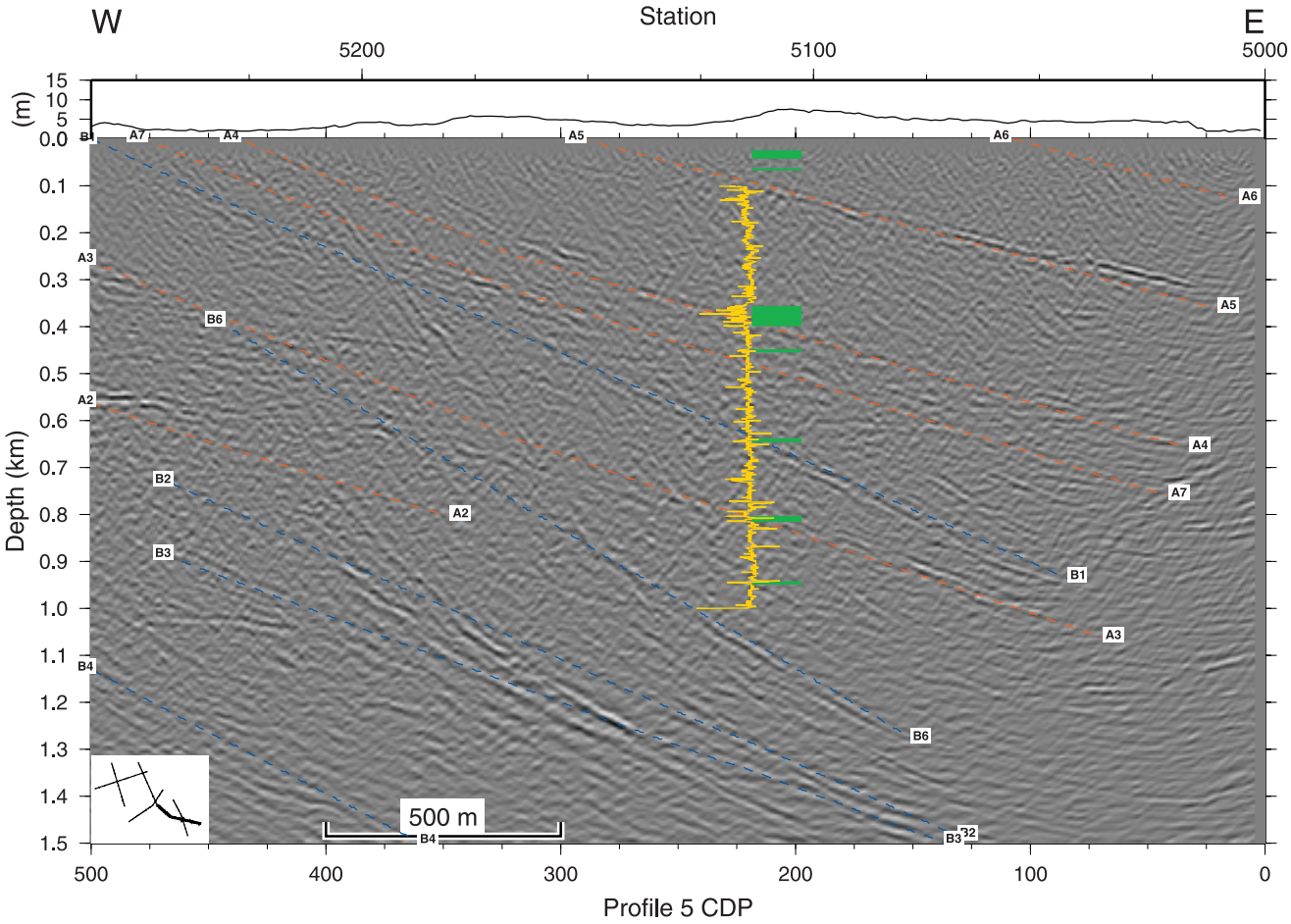

Figure 10. Migrated section of the southeastern part of profile 5. P wave velocity geophysical log from the KFM03A borehole [*Nielsen and Ringgaard*, 2004] is shown in yellow, and fracture zones [*Carlsten et al.*, 2004] are indicated in green. Depths of the selected set A (red) and set B (blue) reflectors have been projected into the section. The depths of these reflectors correspond to the depths where the reflectors would be intersected if a borehole were to be drilled along the profile. They should be viewed as true depths. Migration was done with Kirchhoff depth migration using the DMO velocities with which the stacked section was processed.

since their contact with the surrounding metagranite would act as a plane of weakness.

[32] In summary, we interpret the geometry of the prominent reflections in the southeast to be controlled by the geometry of the generally hydraulically conductive fracture zones, but that amphibolites may locally enhance, perhaps significantly, the amplitude of the reflectivity. Borehole seismics in the KFM03A borehole with offset sources could potentially answer the question of the lateral extent of the amphibolites and determine the exact depths from which reflections are generated.

6.2. Correlation With Topographic Lineaments and Magnetic Anomalies

[33] Moderate to steeply dipping fracture zones appear to control the topography in the Oskarshamn area in southeastern Sweden [*Juhlin and Palm*, 1999; *Bergman et al.*, 2002]. Projection of the set A and B reflections to the surface at Forsmark shows that a few of these reflectors (e.g., A5) appear to correspond to breaks in the topography (Figures 8 and 9), but not to the extent observed in southeastern Sweden. The low topographic relief in the Forsmark area implies that there is considerable uncertainty concerning the recognition and interpretation of topographic lineaments. Larger-scale topographic lows further inland (Figure 1), where the topographic relief is higher, may be related, in some cases, to dipping fracture zones.

[34] Projection of the reflections to the surface shows no correlation with features on the magnetic anomaly map (Figure 12). An irregular magnetic anomaly pattern with higher and lower magnetic areas dominates that part of the site where the reflection seismic survey has been carried out (Figure 12 and *Isaksson et al.* [2004a]). Primary variation in the contents of magnetite in the metagranite, which is reflected in variable magnetic susceptibility values [*Stephens et al.*, 2003b; *Isaksson et al.*, 2004b], can explain much of this pattern. Furthermore, the distinctive low magnetic area that is intersected by several reflectors (e.g., A4, A7, and B1) correlates with a medium-grained metatonalite that shows consistently low magnetic susceptibility values [*Stephens et al.*, 2003b]. This rock type correlates at depth with the metatonalite in the borehole depth interval 220–293 m in KFM03A.

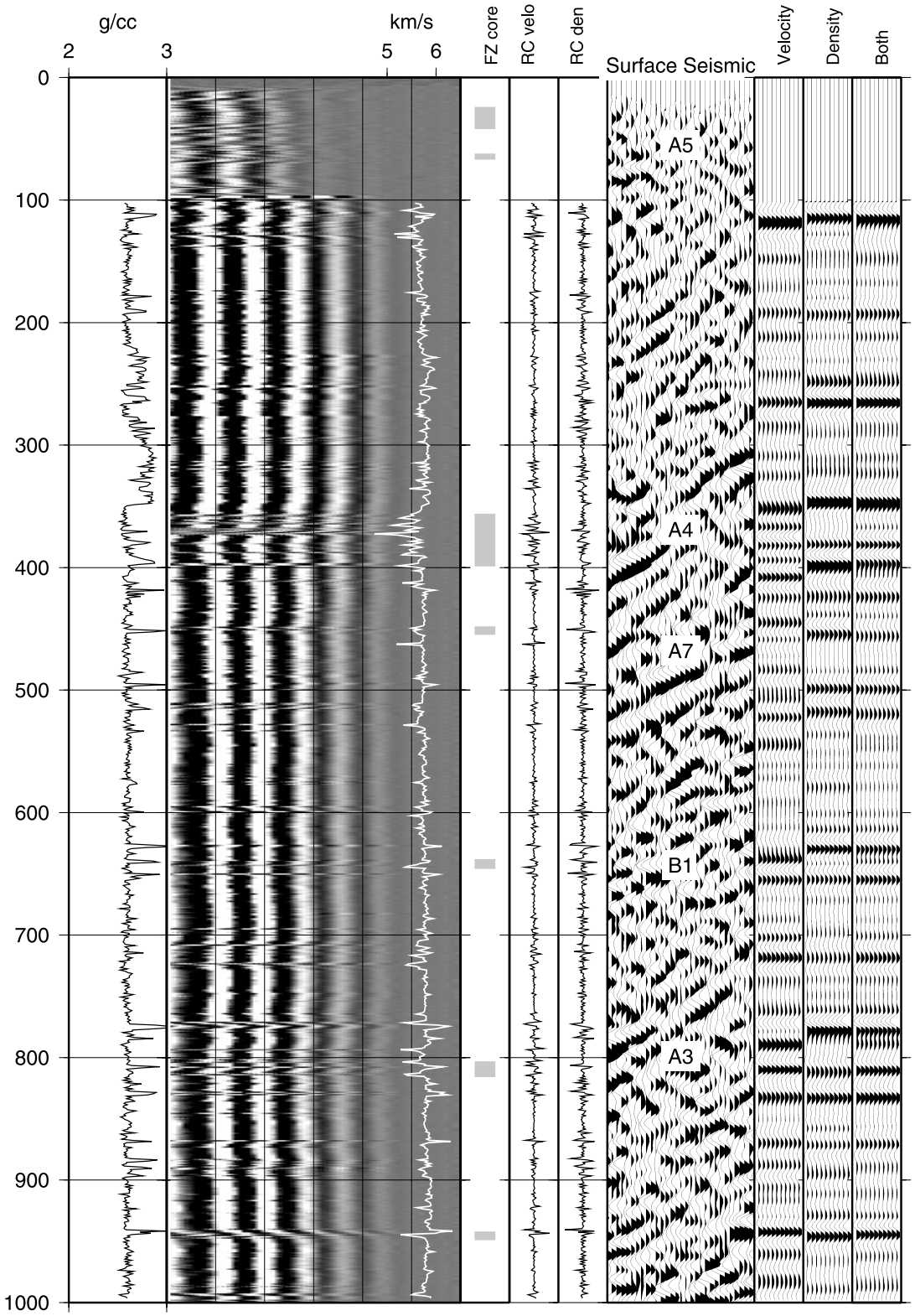

Figure 11. Density and sonic logs from the KFM03A borehole compared to the migrated seismic section along profile 3 and synthetic seismograms. P wave sonic velocity is plotted on top of the full waveform sonic seismograms from the near receiver. Shaded portions in the FZ core panel indicate where the major deformation zones in the core have been identified. Reflection coefficients (RC) have been calculated using only the sonic and only the density log, to allow a comparison of the importance of the contrasts in these two parameters. They are plotted on a scale ranging from −0.1 to 0.1. Synthetic seismograms were generated using a Ricker wavelet corresponding to a peak amplitude at 150 Hz using only the velocity, only the density, and the impedance reflectivity series. Borehole was cased to 100 m.

Table 4. Estimated P Wave Velocities and Densities of Metagranite, Amphibolite, and Fracture Zones Based on Geophysical Log Data From Borehole KFM03A

Rock Type	P Wave Velocity, m/s	Density, kg/m^3	Impedance, kg/m^2 s	Reflection Coefficient Relative to Metagranite
Metagranite	5900	2600	15,340,000	0
Amphibolite	6500	2900	18,850,000	0.10
Fracture zone	5200	2600	13,520,000	−0.06

[35] A suite of low magnetic lineaments that trend in a NE direction and transect the candidate area at Forsmark is a second important feature of the magnetic anomaly map (Figure 12). These lineaments and the surface projection of the reflectors do not correlate with each other (Figure 12). A relationship of these lineaments to the NE set of steeply dipping, minor fracture zones is favored [*SKB*, 2004a, 2005]. In summary, it appears that the features on the magnetic anomaly map, in the area where the reflection seismic survey was carried out, are related to the primary

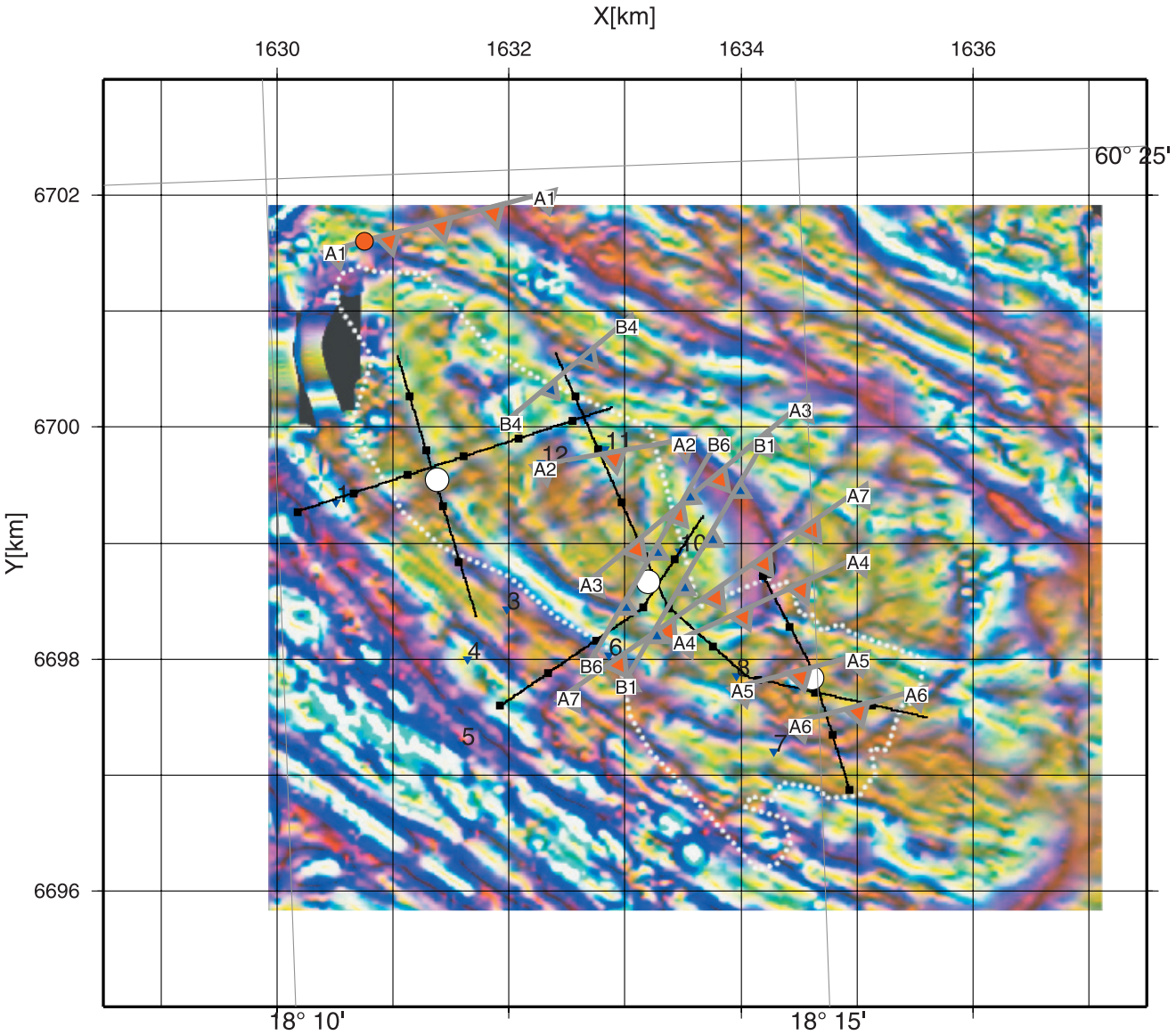

Figure 12. Reflectors projected to the surface and plotted onto the magnetic anomaly map based on data of *Rønning et al.* [2003] and Figure 4-6a of *Isaksson et al.* [2004a]. The lilac areas on the map indicate low magnetic anomalies. White circles mark the locations of the near-vertical cored boreholes KFM01A/KFM01B, KFM02A, and KFM03A/KFM03B. Where the set A and set B reflectors can be traced to the surface, they are marked with the symbol on the downdip side. A red dot marks where the A1 reflector projects to the surface. Small white dots outline the candidate area.

variation of magnetite content in the various rock types and the steeply dipping NE set of fracture zones.

6.3. Orientation of the Singö Deformation Zone and Character of the A1 Reflector

[36] No previous reflection seismic data are available from the Forsmark site. However, during the BABEL project [*BABEL Working Group*, 1993], deep seismic marine data were acquired about 40 km to the north (Figure 1). Apparent, gently to moderately east dipping reflections on the E-W BABEL line 7 in the Bothian Sea and a land based, SERCEL 348 stationary spread that recorded the air gun shots were interpreted [*Law and Snyder*, 1997] as correlating with the Singö shear zone [*Talbot and Sokoutis*, 1988, 1995]. It should be noted that no 3-D control on the orientation of the reflections was available and that the seismic line runs oblique to the Singö shear zone. Therefore the true dip of the reflecting zone may be much steeper. However, the data require a component of easterly dip if the reflections are generated by the Singö shear zone. Given that the Singö shear zone is a major structure, its dip would be expected to have about the same geometry further south at the Forsmark site.

[37] In the present study, the A1 reflector projects to the surface north of profile 4, close to the surface trace of the Singö deformation zone. However, the interpreted strike of the A1 reflector is at an high angle to the Singö zone, implying that the two are not related. Only some weak reflections are observed on the seismic profiles that show strikes consistent with the Singö deformation zone. Given the present data set, we conclude that the Singö deformation zone is either subvertical, as inferred in previous structural models for the Forsmark site [*Axelsson and Hansen*, 1997; *Holmén and Stigsson*, 2001; *SKB*, 2004a, 2005], or has an easterly component of dip, as suggested by *Law and Snyder* [1997].

[38] The A1 reflection shows a more complex pattern of reflectivity than the set A reflections that were penetrated in the KFM03A/KFM03B boreholes. It projects to the surface close to an inhomogeneous rock unit with amphibolite dykes, and, in a ductile manner, more highly deformed rocks. These two observations suggest that the A1 reflection may originate from a more complex geological unit rather than a simple brittle deformation zone. A banded rock unit with amphibolite dykes that is spatially associated with a complex deformation zone that includes mylonites is tentatively suggested. Additional seismic surveying across the Singö deformation zone and more detailed imaging of the A1 reflector will help to determine the orientation of the former, and perhaps, the origin of the latter.

6.4. Tectonic Conditions During Formation of the Gently Dipping Zones

[39] Considerable information is available bearing on the growth and radical reworking of the continental crust in the western part of the Fennoscandian Shield during the Svecokarelian orogeny (1.96 to 1.75 Ga). During this time period, this part of Sweden formed the continental margin to older crustal segments to the north and east [e.g., *Gaál and Gorbatschev*, 1987; *Stephens et al.*, 1992]. Much of the presently exposed crust underwent deformation in the ductile regime, reflecting the thermal and/or depth conditions for this segment of the continental crust during this period. Considerably less information is available concerning the later, intracrustal deformation in the western part of the shield, in eastern Sweden, when the focus of crustal growth, crustal reworking and crustal deformation had shifted southward and westward to younger continental margins. During the long time period from 1.75 Ga up to the present, only far-field effects of the deformation along the newly established continental margins (Table 1) potentially affected the shield in eastern Sweden.

[40] Dextral transpressive strain along ductile deformation zones with WNW and NW strike is an important structural feature of the Svecokarelian tectonic development in the western part of the Fennoscandian Shield [e.g., *Stephens and Wahlgren*, 1996; *Högdahl*, 2000; *Beunk and Page*, 2001; *Persson*, 2002]. The strain along these zones is partitioned with a component of dextral strike-slip displacement along the zones and a component of compression across them. Crustal deformation related to a continent-ocean, oblique collision has been proposed [*SKB*, 2004a]. In this collision, oceanic crust, which moved toward the north to northwest (present-day orientation), collided at different times, along an active continental margin, with an older, Archaean and Early Paleoproterozoic continental nucleus to the northeast.

[41] The regionally important deformation zones at the Forsmark site with WNW strike and steep dip (e.g., Forsmark and Singö deformation zones), which initiated their development in the ductile regime but continued to be active in the brittle regime, are examples of these Svecokarelian, dextral transpressive zones (Figure 13a). Kinematic data are sparse at the site, but ductile high-strain structures that strike in this direction and show a dextral component of movement are present [*Stephens et al.*, 2003a]. It is suggested that the splays of ductile and brittle deformation zones with NW strike (e.g., Eckarfjärden deformation zone) represent second-order synthetic Riedel shears within the strike-slip system (Figure 13a). The steeply dipping NE and NNW sets of fracture zones are suggested to have formed somewhat later in the structural development, as third-order, antithetic and fourth-order, extensional structures, respectively (Figure 13a).

[42] The gently dipping fracture zones with ENE and NE strike, which are represented by the set A and B reflectors, are considered to represent minor thrust faults that are also related to the dextral strike-slip displacement (Figure 13a). In this tectonic model, the gently dipping structures developed during the latest stages of the Svecokarelian orogeny, after cooling had progressed sufficiently for this part of the crust to respond in a brittle manner to the regional stress field. This hypothesis predicts that the gently dipping zones are sandwiched in discrete sets between the important, steeply dipping zones with WNW and NW strike. The significance of post-Svecokarelian tectonic events for reactivation of one or more of the different sets of deformation zones is not addressed here.

[43] Alternative tectonic models for the gently dipping fracture zones treat these structures as far-field responses, in the interior of the craton, to major tectonic events along younger continental margins to the south and west. Only compressional and extensional events that are of major tectonic significance are considered (Table 1). Possible

events include the Gothian, Hallandian, and Sveconorwegian orogenies during the time periods 1.70–1.56, 1.46–1.42 and 1.10–0.90 Ga, respectively, the opening of the Iapetus Ocean during latest Neoproterozoic time, and various Phanerozoic events including the Caledonian orogeny, the Alpine orogeny and the opening of the North Atlantic Ocean during the early Tertiary.

[44] The presence of epidote as a mineral filling along fractures in the gently dipping zones, as well as along the steeply dipping zones with WNW and NW strike (Figure 13a), implies that both sets are old geological structures. Furthermore, a development in the later part of the Svecokarelian orogeny explains, in a consistent manner, a geometric relationship between the gently dipping structures and the different sets of steeply dipping deformation zones. For these two reasons, the Svecokarelian origin hypothesis is favored at the present time, and forms a part of the working, conceptual structural model for the Forsmark site. However, at the present time, there are neither kinematic data for the fractures in the gently dipping zones nor any geochronological data for the mineral fillings or coatings along these fractures. These data are required to more closely constrain hypotheses that can relate these structures to a particular tectonic scenario. On account of these deficiencies, the Svecokarelian model discussed above, or an origin related to the tectonic events mentioned earlier, must be regarded as working hypotheses and are speculative in character at this stage.

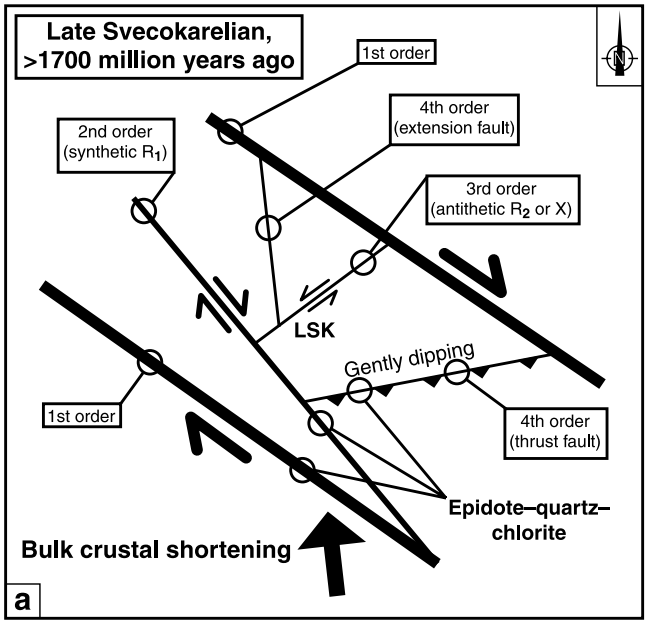

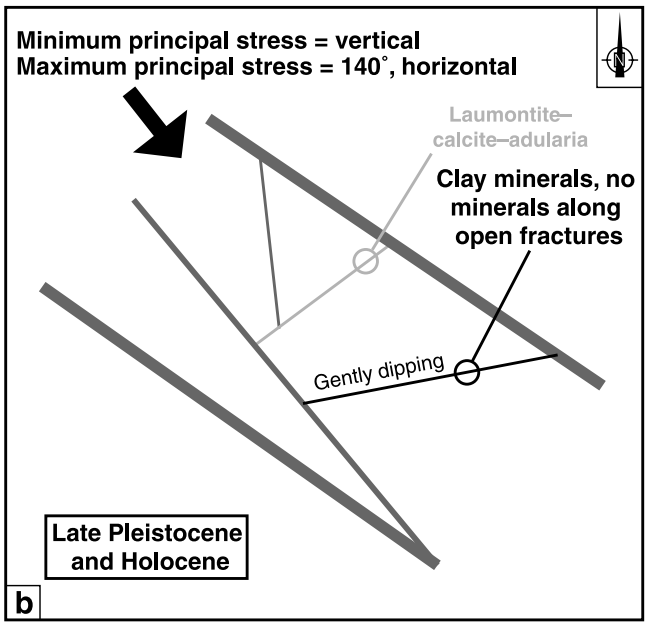

Figure 13. (a) Two-dimensional plan view of the working structural model for the generation of the major sets of brittle deformation zones (WNW and NW, NE, NNW and gently dipping) at the Forsmark site. Only the WNW and NW zones display ductile deformation and all sets, except the fourth-order, minor thrust faults, are steeply dipping. The seismic reflectors correspond to the minor thrust faults. (b) Inferred reactivation of fracture zones in the current stress field, during the late Pleistocene and Holocene. Fractures along the gently dipping fracture zones (black), at a high angle to σ_3, are strongly favored to open as joints in the current stress regime. The precipitation of clay minerals along fractures in these zones as well as the development of open fractures without mineral coatings are also considered to be geologically young features. By contrast, fractures along the steeply dipping zones with NE strike (pale gray shading), perpendicular to the current σ_1, are not favored for aperture development in the current stress field. The laumontite, calcite, and adularia along these fractures were deposited during one or more reactivation events between the time periods shown in Figures 13a and 13b. Fractures along the steeply dipping zones that strike WNW, NW, and NNW (dark gray shading), close to the current σ_1, may also open as joints in the current stress regime.

6.5. Reactivation as Joints in the Current Stress Regime

[45] The gently dipping fracture zones at the Forsmark site are characterized by the occurrence of gently dipping and subhorizontal fractures, many of which are open, as well as high groundwater transmissivity values. In situ stress measurements at the Forsmark site [*Carlsson and Christiansson*, 1987; *SKB*, 2004a, 2005] show that the current, maximum principal stress (σ_1) is subhorizontal with a mean orientation in a NW-SE (140°) direction (Figure 13b). These data also demonstrate that the site is characterized by high rock stresses (average value for σ_1 is 45 MPa at a depth of 500 m, see *SKB* [2005]), which have been related, in part, to the loading effect by Quaternary ice sheets [*Carlsson and Olsson*, 1982]. The current, minimum principal stress (σ_3) is vertical. The implication of these data is that, at shallow crustal levels, the differential stress ($\sigma_1-\sigma_3$) is high. Furthermore, this parameter would have increased significantly, following rapid removal of ice after the latest Weichselian glaciation, during late Pleistocene and Holocene time [*Carlsson*, 1979].

[46] The changes in the stress regime following the latest glaciation event have been invoked to explain the formation of stress release sheet joints in the uppermost (<10 m)

crustal levels at the Forsmark site [*Carlsson*, 1979]. These joints represent reactivated, older subhorizontal fractures. Formation of new fractures with apertures subparallel to the topography is also likely. It is suggested here that the character of the gently dipping zones at deeper crustal levels (at least down to ~1 km) is steered by similar constraints. An important factor is the orientation of the geologically old, gently dipping and subhorizontal fractures, which prevail in the gently dipping zones, at a high angle to the current σ_3 (Figure 13b). A corollary of these considerations is that the steeply dipping NE set of fracture zones at the site, which transect the candidate area and are oriented at a high angle to σ_1, will not be favored for aperture development and groundwater flow in the current stress regime (Figure 13b).

6.6. Implications for the Nuclear Waste Repository

[47] The results from the seismic reflection survey presented here have played an important role in guiding further site investigations at Forsmark. From a safety, construction, and operational point of view, it is desirable to place the repository in an area that contains few hydraulically conductive fracture zones. Hydraulic tests show that the bedrock is considerably more conductive at proposed repository depths (400–500 m) in the southeastern rather than in the northwestern part of the candidate area. Indeed, transmissivity values along these fracture zones, some as high as 10^{-4} m^2/s [*Forsman et al.*, 2004], are considerably above those normally found in crystalline basement. The set A and set B reflections in the southeast are inferred to represent gentle dipping fracture zones that are hydraulically conductive. In the northwestern part of the candidate area, the seismically transparent crust indicates that highly transmissive zones are not present at repository depths. Since the reflection seismic data presented here became available, SKB has decided to continue all the remaining geoscientific studies at the Forsmark site in the northwestern part of the candidate area. Thus the reflection seismic data, in combination with the verifying work presented in the cored borehole data, have steered the subsequent focus in geoscientific studies at the site.

7. Conclusions

[48] The reflection seismic surveying to date shows a marked contrast in the reflectivity pattern between the northwestern and southeastern parts of the Forsmark site. Clear, gently dipping reflections in the uppermost 1–2 km characterize the images from the southeast. Drilling results show that these gently dipping reflections are associated with fracture zones. Smaller lenses of amphibolite within these zones may enhance the reflectivity. In contrast, the upper 1–2 km is nearly transparent in the northwest, apart from the more steeply dipping A1 reflection. Here, drilling results show that the bedrock is relatively homogeneous and contains a generally low frequency of fractures. The reflection seismic data, in combination with the verifying work presented in the cored borehole data, have steered the subsequent focus in geoscientific studies to the northwestern part of the site.

[49] The A1 reflection projects up into the Singö shear zone, but has a different orientation. The present survey has not imaged the Singö shear zone, indicating that it is either steeply dipping or has an easterly dip component as suggested in previous studies. Although not confirmed yet, the gently dipping structures in the southeast may be laterally limited by steeply dipping, ductile and brittle deformation zones that surround the tectonic lens at Forsmark and that strike WNW and NW. Some of the gently dipping reflections project to the surface close to topographic anomalies, but most show no clear correlation with topography.

[50] Although kinematic and geochronological data are lacking from the gently dipping fracture zones, the mineralogy along the fractures in these zones, as well as their geometric relationship to the steeply dipping structures, suggest that they formed during the waning stages of the Svecokarelian orogeny. In this working model, the gently dipping zones are inferred to have formed as minor thrusts within a regionally significant, dextral strike-slip fault system. However, the character of the fracture mineralogy indicates one or more phases of later reactivation. It is suggested that the occurrence of open fractures and the presence of groundwater along these zones is related to an intimate interplay between the present orientation of principal stresses, the high intensity of gently dipping and subhorizontal fractures along the zones, the high in situ stresses in the bedrock, and rapid unloading after the latest Weichselian glaciation. Removal of the ice sheet gave rise to a high differential stress, especially at shallow crustal levels. In this situation, older fractures along the gently dipping zones would have opened as joints and, especially at the uppermost crustal levels, even new stress release sheet joints could have formed.

[51] **Acknowledgments.** We thank the Swedish Nuclear Waste Management Co. (SKB) and, in particular, Kaj Ahlbom for their support in this project and for the permission to publish this paper. We are also grateful to Hans Isaksson (GeoVista AB) for help with the production of Figure 12. The Associate Editor, Sandy Steacy, and two anonymous reviewers are thanked for their critical reviews that helped improve this paper.

References

Ayarza, P., et al. (2000), Integrated geological and geophysical studies in the SG4 borehole area, Tagil Volcanic Arc, Middle Urals: Location of seismic reflectors and source of the reflectivity, *J. Geophys. Res.*, *105*, 21,333–21,352.

Axelsson, C.-L., and L. M. Hansen (1997), Update of structural models at SFR nuclear waste repository, Forsmark, Sweden, *SKB Rep. R-98-05*, 43 pp., Swed. Nucl. Fuel and Waste Manage. Co., Stockholm. (Available at http://www.skb.se)

BABEL Working Group (1993), Integrated seismic studies of the Baltic Shield using data in the Gulf of Bothnia region, *Geophys. J. Int.*, *112*, 305–324.

Bergman, B., C. Juhlin, and H. Palm (2002), Reflection seismic imaging of the upper 4 km of crust using small charges (15–75 grams) at Laxemar, southeastern Sweden, *Tectonophysics*, *355*, 201–213.

Beunk, F. F., and L. M. Page (2001), Structural evolution of the accretional continental margin of the Paleoproterozoic Svecofennian orogen in southern Sweden, *Tectonophysics*, *339*, 67–92.

Carlsson, A. (1979), Characteristic features of a superficial rock mass in southern central Sweden. Horizontal and subhorizontal fractures and filling material, *Striae*, *11*, 1–79.

Carlsson, A., and R. Christiansson (1987), Geology and tectonics at Forsmark, Sweden, *SKB Rep. SFR 87-04*, 91 pp., Swed. Nucl. Fuel and Waste Manage. Co., Stockholm.

Carlsson, A., and T. Olsson (1982), High rock stresses as a consequence of glaciation, *Nature*, *298*, 739–742.

Carlsten, S., J. Petersson, M. B. Stephens, H. Thunehed, and J. Gustafsson (2004), Forsmark site investigation. Geological single-hole interpretation of KFM03B, KFM03A and HFM06–08 (DS3), *SKB Rep. P-04-118*,

41 pp., Swed. Nucl. Fuel and Waste Manage. Co., Stockholm. (Available at http://www.skb.se)

Claesson, L.-Å., and G. Nilsson (2004), Forsmark site investigation. Drilling of the telescopic borehole KFM03A and the core drilled borehole KFM03B at drilling site DS3, *SKB Rep. P-03-59*, 80 pp., Swed. Nucl. Fuel and Waste Manage. Co., Stockholm. (Available at http://www.skb.se)

Cosma, C., L. Balu, and N. Enescu (2003), Estimation of 3D positions and orientations of reflectors identified in the reflection seismic survey at the Forsmark area, *SKB Report R-03–22*, 88 pp., Swed. Nucl. Fuel and Waste Manage. Co., Stockholm. (Available at http://www.skb.se)

Coward, M. P., D. Dietrich, and R. G. Park (1989), *Alpine Tectonics*, *Geol. Soc. Spec. Publ.*, *45*, 450 pp.

Forsman, I., M. Zetterlund, and I. Rhén (2004), Correlation of Posiva Flow Log anomalies to core mapped features in Forsmark (KFM01A to KFM05A), *SKB Report R-04-77*, 446 pp., Swed. Nucl. Fuel and Waste Manage. Co., Stockholm. (Available at http://www.skb.se)

Gaál, G., and R. Gorbatschev (1987), An outline of the Precambrian evolution of the Baltic Shield, *Precambrian Res.*, *35*, 15–52.

Gee, D. G., and B. A. Sturt (1985), *The Caledonide Orogen Scandinavia and Related Areas*, 1266 pp., John Wiley, Hoboken, N. J.

Gustafsson, J., and J. Gustafsson (2004), Forsmark site investigation. RAMAC and BIPS logging in borehole KFM03A and KFM03B, *SKB Rep. P-04-41*, 92 pp., Swed. Nucl. Fuel and Waste Manage. Co., Stockholm. (Available at http://www.skb.se)

Högdahl, K. (2000), Late-orogenic, ductile shear zones and protolith ages in the Svecofennian Domain, central Sweden, *Medd. Stockholms Univ. Inst. Geol. Geokemi*, *309*, 1–21.

Holmén, J. G., and M. Stigsson (2001), Modelling of future hydrogeological conditions at SFR, *SKB Rep. R-01-02*, 285 pp., Swed. Nucl. Fuel and Waste Manage. Co., Stockholm. (Available at http://www.skb.se)

Isaksson, H., H. Thunehed, and M. Keisu (2004a), Forsmark site investigation: Interpretation of airborne geophysics and integration with topography: Stage 1(2002), *SKB Rep. P-04-29*, 71 pp., Swed. Nucl. Fuel and Waste Manage. Co., Stockholm. (Available at http://www.skb.se)

Isaksson, H., H. Mattsson, H. Thunehed, and M. Keisu (2004b), Forsmark site investigation. Interpretation of petrophysical data. Stage 1(2002), *SKB Rep. P-03-102*, 81 pp., Swed. Nucl. Fuel and Waste Manage. Co., Stockholm. (Available at http://www.skb.se)

Juhlin, C. (1990), Interpretation of the reflections in the Siljan Ring area based on results from the Gravberg-1 borehole, *Tectonophysics*, *173*, 345–360.

Juhlin, C. (1995), Imaging of fracture zones in the Finnsjön area, central Sweden, using the seismic reflection method, *Geophysics*, *60*, 66–75.

Juhlin, C., and B. Bergman (2004), Reflection seismics in the Forsmark area: Updated interpretation of stage 1 (previous report R-02-43), updated estimate of bedrock topography (previous report P-04-99), *SKB Rep. P-04-158*, 25 pp., Swed. Nucl. Fuel and Waste Manage. Co., Stockholm. (Available at http://www.skb.se)

Juhlin, C., and H. Palm (1999), 3D structure below Ävrö island from high resolution reflection seismic studies, southeastern Sweden, *Geophysics*, *64*, 662–667.

Juhlin, C., B. Bergman, and H. Palm (2002), Reflection seismic studies in the Forsmark area - stage 1, *SKB Rep. R-02-43*, 63 pp., Swed. Nucl. Fuel and Waste Manage. Co., Stockholm. (Available at http://www.skb.se)

Juhlin, C., B. Bergman, H. Palm, and A. Tryggvason (2004), Oskarshamn site investigation: Reflection seismic studies on Ävrö and Simpevarpshalvön, 2003, *SKB Rep. P-04-52*, 49 pp., Swed. Nucl. Fuel and Waste Manage. Co., Stockholm. (Available at http://www.skb.se)

Law, A., and D. B. Snyder (1997), Reflections from a mylonitized zone in central Sweden, *J. Geophys. Res.*, *102*, 8411–8425.

Mair, J., and A. Green (1981), High-resolution seismic reflection profiles reveal fracture zones within a "homogeneous" granite batholith, *Nature*, *294*, 439–442.

Nedimovic, M. R., and G. F. West (2002), Shallow three-dimensional structure from two-dimensional crooked line seismic reflection data over the sturgeon lake volcanic complex, *Econ. Geol.*, *97*, 1779–1794.

Nedimovic, M. R., and G. F. West (2003), Crooked-line 2D seismic reflection imaging in crystalline terrains: part 2, Migration, *Geophysics*, *68*, 286–296.

Nielsen, U. T., and J. Ringgaard (2004), Forsmark site investigation: Geophysical borehole logging in borehole KFM02A, KFM03A and KFM03B, *SKB Rep. P-04-97*, 57 pp., Swed. Nucl. Fuel and Waste Manage. Co., Stockholm. (Available at http://www.skb.se)

Page, L., T. Hermansson, P. Söderlund, J. Andersson, and M. B. Stephens (2004), Forsmark site investigation. Bedrock mapping. U-Pb, $^{40}Ar/^{39}Ar$ and (U-Th)/He geochronology, *SKB Report P-04-126*, 64 pp., Swed. Nucl. Fuel and Waste Manage. Co., Stockholm. (Available at http://www.skb.se)

Persson, K. S. (2002), Deformation zones in models and nature, *Comprehensive Summ. Uppsala Diss. 788*, 58 pp., Fac. Sci. and Technol., Uppsala Univ., Uppsala.

Petersson, J., A. Wängerud, P. Danielsson, and A. Ståhle (2004), Forsmark site investigation: Boremap mapping of telescopic drilled borehole KFM03A and core drilled borehole KFM03B, *SKB Rep. P-03-116*, 55 pp., Swed. Nucl. Fuel and Waste Manage. Co., Stockholm. (Available at http://www.skb.se)

Rønning, H. J. S., O. Kihle, J. O. Mogaard, P. Walker, H. Shomali, P. Hagthorpe, S. Byström, H. Lindberg, and H. Thunehed (2003), Forsmark site investigation. Helicopter-borne geophysics at Forsmark, Östhammar, Sweden, *SKB Rep. P-03-41*, 137 pp., Swed. Nucl. Fuel and Waste Manage. Co., Stockholm. (Available at http://www.skb.se)

Sandström, B., M. Savolainen, and E.-L. Tullborg (2004), Forsmark site investigation. Fracture mineralogy. Results from fracture minerals and wall rock alteration in boreholes KFM01A, KFM02A, KFM03A and KFM03B, *SKB Rep. P-04-149*, 93 pp., Swed. Nucl. Fuel and Waste Manage. Co., Stockholm. (Available at http://www.skb.se)

Swedish Nuclear Fuel and Waste Management Co. (SKB) (2001), Site investigations: Investigation methods and general execution programme, *SKB Rep. TR-01-29*, 264 pp., Stockholm. (Available at http://www.skb.se)

Swedish Nuclear Fuel and Waste Management Co. (SKB) (2004a), Preliminary site description: Forsmark area, version 1.1, *SKB Rep. R-04-15*, 399 pp., Stockholm. (Available at http://www.skb.se)

Swedish Nuclear Fuel and Waste Management Co. (SKB) (2004b), Preliminary site description: Simpevarp area, version 1.1, *SKB Rep. R-04-25*, 465 pp., Stockholm. (Available at http://www.skb.se)

Swedish Nuclear Fuel and Waste Management Co. (SKB) (2005), Preliminary site description: Forsmark area, version 1.2, *SKB Rep. R-05-18*, 752 pp., Stockholm. (Available at http://www.skb.se)

Stephens, M. B. (1988), The Scandinavian Caledonides: A complexity of collisions, *Geol. Today*, *4*, 20–26.

Stephens, M. B., and C.-H. Wahlgren (1996), Post-1.85 Ga tectonic evolution of the Svecokarelian orogen with special reference to central and SE Sweden (extended abstract), *GFF*, *118*, A26–A27.

Stephens, M. B., C.-H. Wahlgren, and P. Weihed (1992), Sweden, in *Encyclopedia of European and Asian Regional Geology*, edited by E. M. Moores and R. W. Fairbridge, pp. 690–704, CRC Press, Boca Raton, Fla.

Stephens, M. B., S. Lundqvist, T. Bergman, J. Andersson, and M. Ekström (2003a), Forsmark site investigation: Bedrock mapping: Rock types, their petrographic and geochemical characteristics, and a structural analysis of the bedrock based on Stage 1(2002) surface data, *SKB Rep. P-03-75*, 133 pp., Swed. Nucl. Fuel and Waste Manage. Co., Stockholm. (Available at http://www.skb.se)

Stephens, M. B., T. Bergman, J. Andersson, T. Hermansson, C.-H. Wahlgren, L. Albrecht, and H. Mikko (2003b), Forsmark site investigation. Bedrock mapping. Stage 1(2002) –Outcrop data including fracture data, *SKB Rep. P-03-09*, 23 pp., Swed. Nucl. Fuel and Waste Manage. Co., Stockholm. (Available at http://www.skb.se)

Talbot, C. J., and D. Sokoutis (1988), The Singö shear zone near Östhammar, eastern Sweden, *UUDMP Res. Rep. 55*, 55 pp., Uppsala Univ., Uppsala.

Talbot, C. J., and D. Sokoutis (1995), Strain ellipsoids from incompetent dykes: application to volume loss during mylontization in the Singö gneiss zone, central Sweden, *J. Struct. Geol.*, *17*, 927–948.

Thunehed, H. (2004), Forsmark site investigation. Interpretation of borehole geophysical measurements in KFM02A, KFM03A, KFM03B and HFM04 to HFM08, *SKB Rep. P-04-98*, 51 pp., Swed. Nucl. Fuel and Waste Manage. Co., Stockholm. (Available at http://www.skb.se)

Wiklund, S. (2002), Digitala ortofoton och höjdmodeller: Redovisning av metodik för platsundersökningsområdena Oskarshamn och Forsmark samt förstudieområdet Tierp Norra, *SKB Rep. P-02-02*, 28 pp., Swed. Nucl. Fuel and Waste Manage. Co., Stockholm. (Available at http://www.skb.se)

Wu, J., and R. F. Mereu (1992), Crustal structure of Kapuskasing uplift from LITHOPROBE near-vertical/wide-angle seismic reflection data, *J. Geophys. Res.*, *97*, 17,441–17,453.

Yilmaz, Ö. (1987), *Seismic Data Processing*, Soc. of Explor. Geophys., Tulsa, Okla.

Zalewski, E., D. Eaton, B. Milkereit, B. Roberts, M. Salisbury, and L. Petrie (1997), Seismic reflections from subvertical dikes in Archean terrane, *Geology*, *25*, 707–710.

Ziegler, P. A. (1987), Late Cretaceous and Cenozoic intra-plate compressional deformations in the Alpine foreland a geodynamic model, *Tectonophysics*, *137*, 389–420.

C. Juhlin, Department of Earth Sciences, Uppsala University, Villavägen 16, SE-752 36, Uppsala, Sweden. (christopher.juhlin@geo.uu.se)

M. B. Stephens, Geological Survey of Sweden, Box 670, SE-751 28 Uppsala, Sweden.